Precambrian Research 237 (2013) 36–50

Contents lists available at ScienceDirect

Precambrian Research

journal homepage: www.elsevier.com/locate/precamres

Evidence for 2.0 Ga continental microbial mats in a paleodesert setting

Edward L. Simpson[a,*], Elizabeth Heness[a], Adam Bumby[b], Patrick G. Eriksson[b], Kenneth A. Eriksson[c], Hannah L. Hilbert-Wolf[d], Sarah Linnevelt[b], H. Fitzgerald Malenda[a], Tshepiso Modungwa[b], O.J. Okafor[b]

[a] Department of Physical Sciences, Kutztown University of Pennsylvania, Kutztown, PA 19530, USA
[b] Department of Geology, University of Pretoria, Pretoria 0002, South Africa
[c] Department of Geosciences, Virginia Tech, Blacksburg, VA 24061, USA
[d] School of Earth and Environmental Sciences, James Cook University, Townsville, Qld 4811, Australia

ARTICLE INFO

Article history:
Received 11 March 2013
Received in revised form 3 August 2013
Accepted 7 August 2013
Available online 4 September 2013

Keywords:
Paleoproterozoic
South Africa
Paleo-desert deposits
Microbial mats
Microbially induced sedimentary structures

ABSTRACT

Early evolved microbial communities characterized the initial biological invasion of Precambrian continental landscapes. In modern arid settings, microbial mats and biological soil crusts are well-developed and stabilize sediment. The Paleoproterozoic Makgabeng Formation in South Africa is one of the oldest and best preserved, dryland systems on Earth. Six types of microbial mat-related structures are now recognized within these depositional systems. This paper presents three newly discovered structures that include tufted microbial mat, biological soil crusts, and gas-escape features, in addition to three previously documented structures that include roll up features, sand cracks, and wrinkled features. These discoveries demonstrate that microbial communities were well-established and inhabited diverse continental settings by 2.0 Ga, approximately 200 million years after the onset of the Great Oxidation Event.

1. Introduction

Microbial mat communities played a critical role in the initial biological invasion of Precambrian continental landscapes (Campbell, 1979; Buick, 1992; Prave, 2002; Battistuzzi et al., 2004; Retallack, 2008; Beraldi-Campesi et al., 2009; Beraldi-Campesi and Garcia-Pichel, 2011; Finkelstein et al., 2010; Noffke, 2010; Sheldon, 2012). Stable isotope and/or major element geochemistry gleaned from paleosols and marine sediments have been cited as proxy evidence of initial biological expansion of microbes onto continents in the Archean (Kenny and Knauth, 1992; Gutzmer and Beukes, 1998; Watanabe et al., 2000; Retallack, 2001; Stüeken et al., 2012). During the Archean, this ecospace exploitation led to the initial appearance of the mature quartz sandstones generated partially (in addition to an aggressive paleo-atmosphere) by microbial binding that enhanced in situ weathering (Dott, 2003). Although the exact timing is uncertain, initial terrestrial mat and crust development appear to have occurred after the onset of the prokaryotic radiation (Labandeira, 2005). Phylogenic analysis is congruent with these estimates that colonization of continents transpired between ~2.8 and 3.1 Ga (Battistuzzi et al., 2004).

This study describes the variety of microbially induced sedimentary structures (MISS; Noffke et al., 1996) and biological soil crust (BSC) features in the ~2.0 Ga (new age constraint), Makgabeng Formation, South Africa (Fig. 1) and documents their morphological varieties in continental environments. These MISS and BSC structures signal the presence of a robust and thriving Paleoproterozoic continental microbial ecosystem, approximately 200 million years after the Great Oxidation Event (e.g., Holland, 2002, 2006).

2. Geologic setting

The Waterberg Group ranges from approximately 2.06–1.88 Ga based on new mapping and radiometric age constraints; these age constraints are significantly older than previously thought (SACS, 1980; Jansen, 1982; Walraven and Hattingh, 1993; Bumby, 2000; Bumby et al., 2001, 2004; Eglington and Armstrong, 2004; Hanson et al., 2004; Dorland et al., 2006). The Main Waterberg Basin, part of the Kaapvaal Craton, is bounded to the north by the Limpopo Mobile Belt as exemplified by the Palala Shear Zone (Fig. 1; Light, 1982; Roering et al., 1992; Kröner et al., 1999) and to the south by the Thabazimbi-Murchison lineament (Kröner et al., 1999). The Limpopo Belt has an extended and complex tectonic history with numerous periods of fault reactivation that acted as a northern source for pulses of sediment entering and filling the Waterberg Basin (Bumby, 2000; Bumby et al., 2001, 2004). Regional

* Corresponding author. Tel.: +1 610 698 5031; fax: +1 610 683 1352.
E-mail address: simpson@kutztown.edu (E.L. Simpson).

0301-9268/$ – see front matter © 2013 Elsevier B.V. All rights reserved.
http://dx.doi.org/10.1016/j.precamres.2013.08.001

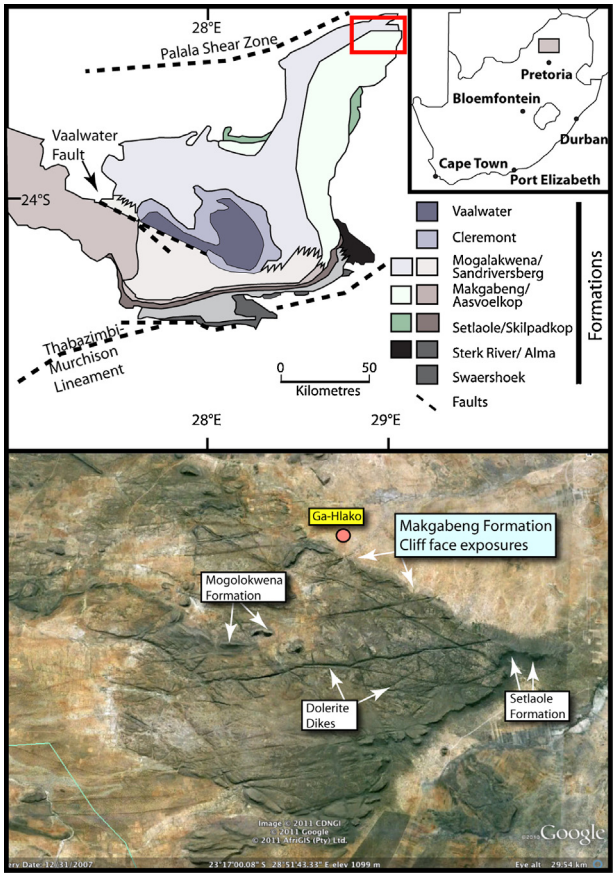

Fig. 1. (A) Locality map of the Main Waterberg Basin in northern South Africa. The northern boundary of the basin is delineated by the Palala Shear Zone and the southern boundary by the Thabazimbi-Murchison Lineament. (B) Google Earth map view of the Makgabeng plateau. Note the location of the cliff exposure and the dip slope to the southwest.

paleocurrent analysis in the northern part of the Waterberg basin supports a consistent source from the Limpopo Belt for the time span of the Waterberg Group fluvial systems (Callaghan et al., 1991; Bumby, 2000; Bumby et al., 2001, 2004; Eriksson et al., 2006, 2008).

Within the Main Waterberg Basin, the Waterberg Group is subdivided into eleven formations that vary vertically and laterally in lithology (Fig. 2; Eriksson et al., 2006). In the northern part of the Main Waterberg Basin the Makgabeng Formation conformably overlies the Setlaole Formation and in turn is disconformably overlain by the Mogalakwena Formation (Fig. 2; SACS, 1980; Jansen, 1982; Bumby, 2000). The Setlaole Formation consists of feldspathic sandstones and conglomerates (with minor volcanic ash layers) that record southward-draining braided fluvial systems shed off the reactivated Limpopo Belt (Fig. 2; Callaghan et al., 1991; Bumby, 2000; Bumby et al., 2001). The contact between the Setlaole and Makgabeng Formations is not well exposed in the study area. Polymictic conglomerates and feldspathic to lithic sandstones characterize the younger Mogalakwena Formation and these reflect the presence of braided stream systems with unusually high stream gradients, also sourced from the reactivated Limpopo Belt (Eriksson et al., 2006, 2008).

The Makgabeng Formation crops out along a series of cliff faces, ~15 km long, as well as dip slope exposures on the concomitant plateau in the northern part of the main basin (Fig. 1; Bumby, 2000; Eriksson et al., 2008) where the Makgabeng Formation reaches a maximum thickness of ~800 m. Here, the upper strata of the Makgabeng Formation are best exposed. The Makgabeng Formation is composed predominately of fine- to medium-grained, quartz-rich sandstone (Callaghan et al., 1991; Eriksson and Cheney, 1992; Bumby, 2000; Eriksson et al., 2000; Simpson et al., 2002, 2004). Along the plateau and the cliff face, strata dip approximately southwest at less than 5°. Metamorphism of the Makgabeng Formation strata was minimal and is mainly linked to a series of cross-cutting, post-Bushveld-age doleritic dikes (Hanson et al., 2004) and shallow-burial metamorphism. The dikes are expressed as a series of linear topographic lows on the plateau (Fig. 1). Hydrothermal metamorphism and soft-sediment deformation of the Makgabeng Formation strata are restricted to the proximity of these dikes.

The Makgabeng Formation quartz sandstones are one of the oldest eolian erg deposits preserved on Earth (Eriksson and Cheney, 1992; Eriksson and Simpson, 1998; Simpson et al., 2002, 2004; Eriksson et al., 2013). Associated with the preserved dune deposits are interdune, saline pan/playa, and minor fluvial environments (Fig. 3; Meinster and Tickell, 1975; Callaghan et al., 1991; Bumby, 2000; Simpson et al., 2002, 2004). Within the eolian deposits, specifically the interdune setting, mudstone roll-up structures have been previously documented (Eriksson et al., 2000, 2007; Porada and Eriksson, 2009). Other types of sedimentary features that are attributable to the binding of microbial mats have been recognized (Eriksson et al., 2007; Porada and Eriksson, 2009). The upper strata of the Makabeng Formation are best exposed within the cliff face and on the dip slopes of the plateau (Meinster and Tickell, 1975; Callaghan et al., 1991; Bumby, 2000; Eriksson et al., 2000; Simpson et al., 2002, 2004; Heness et al., 2012). This work was restricted to the uppermost ~75 m of strata (Fig. 4).

3. Paleoenvironments

The facies composing the upper strata of the Makgabeng Formation record the impact of climate variation on the Paleoproterozic dune field system (Eriksson et al., 2013; Heness et al., 2012). Within this upper portion of the Makgabeng Formation, lower and upper erg deposits are separated by a laterally extensive playa deposit (Figs. 3A and 4 and Table 1; Bumby, 2000; Heness et al., 2012). Variable size sets of eolian cross-strata compose the lower erg deposits (Table 1). Wet interdune deposits of the lower erg increase in abundance, thickness, and lateral extent approaching the overlying medial playa strata (Figs. 3B and 4; Eriksson et al., 2000; Heness et al., 2012). The transition from the lower erg to the overlying playa deposit is abrupt, and the stratal surface at the base of the playa has up to ~50 cm of relief (Fig. 3C). The playa facies varies greatly in grain size, from mudstone to coarse-grained sandstone (Simpson et al., 2004, 2012). Climatic amelioration at variable time scales is reflected in the vertical variation of the facies stacking patterns. The upper erg deposit consists of larger-scale cross-bed sets (Table 1). In the main portion of the upper erg deposit interdune deposits are very thin, less than a centimeter thick, to absent (Fig. 3D). Near the top of the upper erg deposit, playa and interfingering sand-dominated ephemeral fluvial facies reflect an increase in precipitation (Fig. 4; Bumby, 2000; Heness et al., 2012). Also, near the top of the upper erg deposit, dune facies with interbedded massive sandstone facies, more prevalent and better developed below the contact with the overlying Mogalakwena Formation, attest to climatic amelioration that led to cessation of erg development (Fig. 4).

4. Microscopic mat features: establishing biogenicity

Noffke (2009) developed six criteria to determine the biogenicity of sedimentary features found in Precambrian strata. Although the criteria were developed for marine strata, the benchmarks are mostly applicable to Precambrian continental strata as well. Noffke's (2009) criteria necessary to assign biogenicity to features

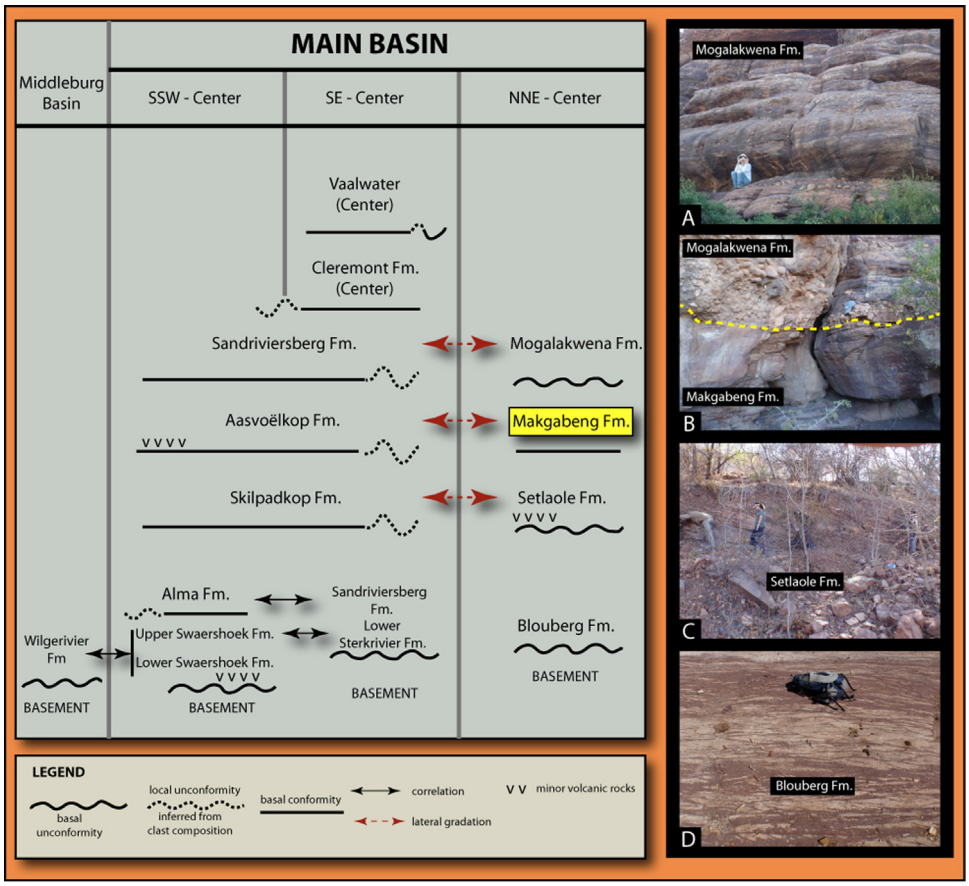

Fig. 2. Stratigraphic units of the Main Waterberg Basin. Chart – Correlation chart of stratigraphic units contained in the Main Waterberg Basin with those of the Middleburg Basin (modified from Eriksson et al., 2008). The stratigraphic interval on which this study is based is exposed in the N–NE of the basin. (A) Conglomerates in the lower part of the Mogalakwena Formation. Person is 1.70 m tall. (B) Erosional contact between the Makgabeng Formation (eolian sandstones) and the younger Mogalakwena Formation (fluvial conglomerates). Hat is ~25 cm. (C) Fluvial sandstones of the Setaole Formation. Person is 1.70 m tall. (D) Fluvial, trough cross bedded sandstones of the Blouberg Formation. Backpack for scale.

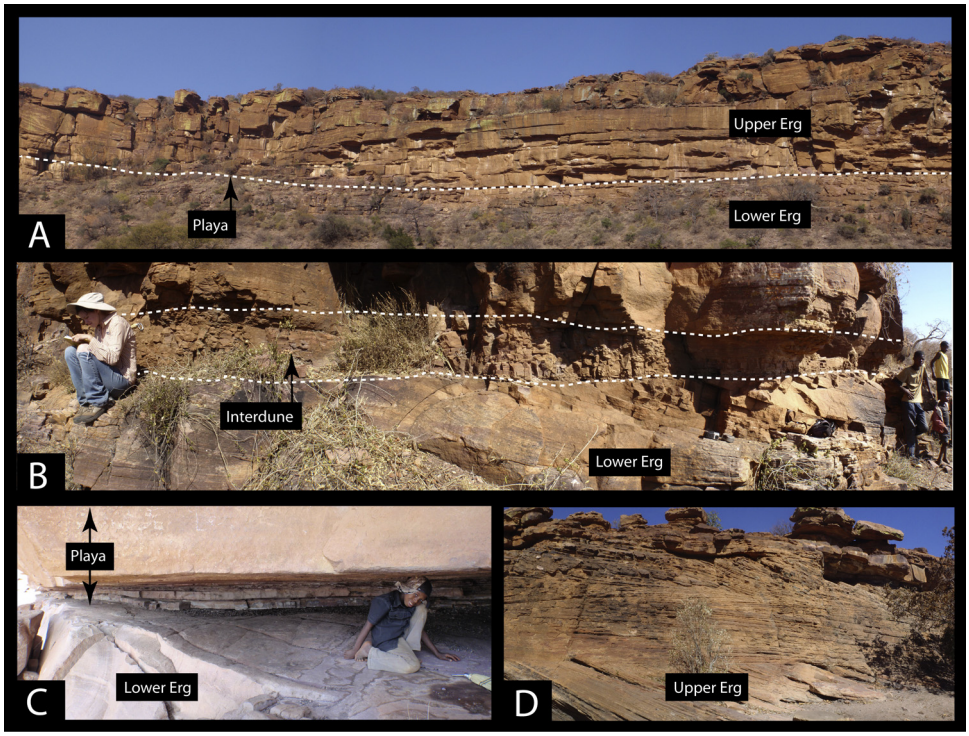

Fig. 3. Field photographs of various facies of the Makgabeng Formation. (A) Cliff face mosaic of the Makgabeng Formation. (B) Photomosaic of lower erg interdune deposits. Note the pinching of interdune deposits laterally to the right of the photo. Figure is 1.7 m tall.

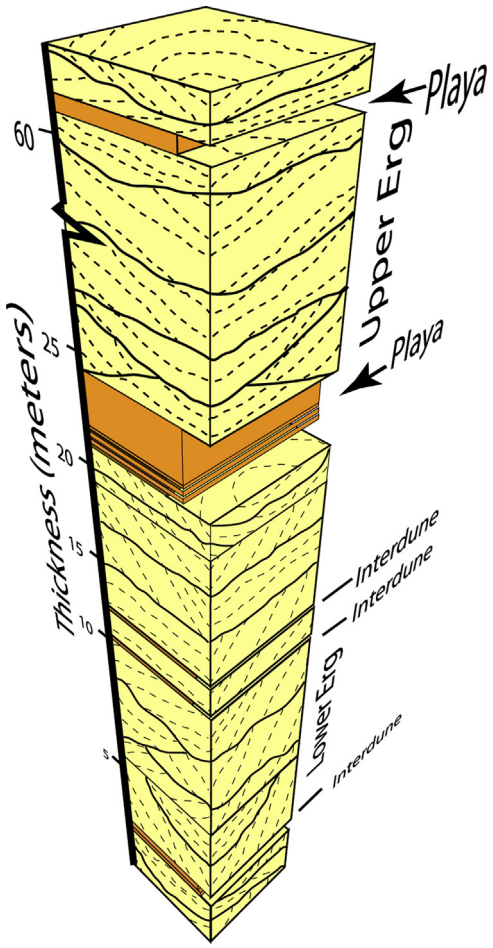

Fig. 4. Composite stratigraphic section through the upper Makgabeng Formation. This section was compiled from 4 measured sections through the lower cliff face. The thickness of the upper erg deposit was estimated by use of GPS.

include: (1) strata with a metamorphic grade less than lower greenschist facies; (2) position in the stratigraphic section that corresponds to the transition from regression to transgression in marine sections (not applicable to true continental settings); (3) interpreted depositional facies that enhance the development and preservation of microbial mats; (4) feature distribution that correlates to the average hydraulic pattern; (5) geometries and patterns that have modern analogs; and (6) presence of, at minimum, one of nine specific microtextures. Microtextural criteria to aid in the identification of mat features include elongate laminae, laminae forming carpet-like textures, fossil fabric orientations matching the modern, ~45° span, and laminations composed of iron oxides and hydroxides, titanium oxides, chlorite, and carbon (Noffke et al., 2008). Schieber (1998) asserts that positive identification requires that microbial filaments be found in thin section in life position.

Deformation is minimal in the Makgabeng Formation (Fig. 5). Makgabeng Formation microbial mat microscopic textures satisfy most of the criteria outlined in Noffke et al. (2008) including filmentous laminae, oriented grains, textures lined with iron oxides and hydroxides and clay minerals (Fig. 5).

5. Mat features in Makgabeng Formation

Mat features, in particular muddy roll-up structures, were first described by Eriksson et al. (2000). Eriksson et al. (2007) and Porada and Eriksson (2009) expanded the list of mat structures by describing sandcracks and wrinkle structures. Three new features

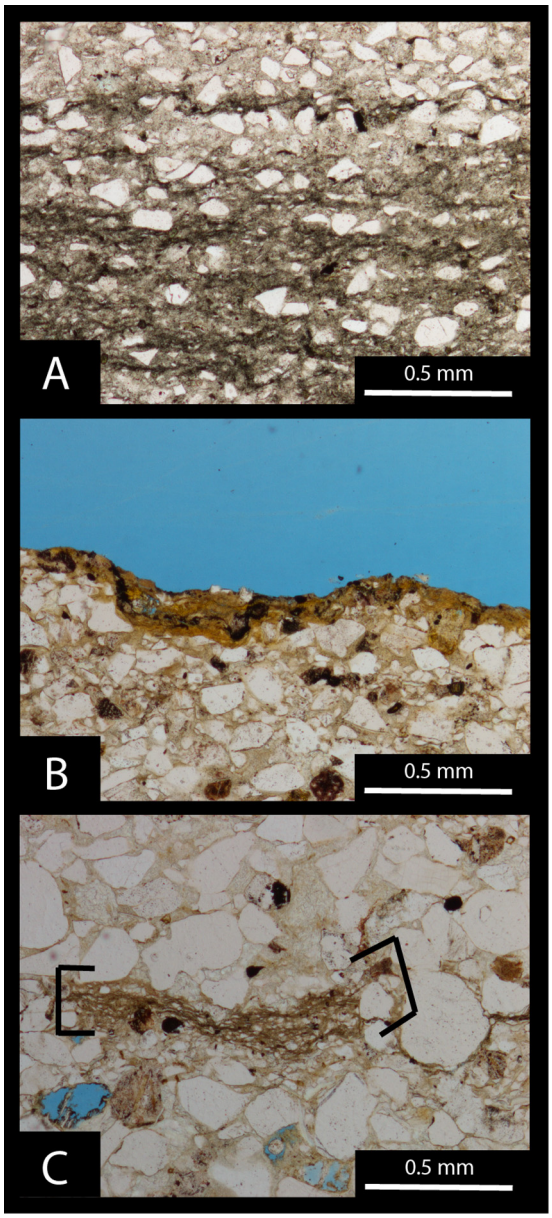

Fig. 5. Photomicrographs of microbial mat features. (A) MISS from marginal marine deposits of the 3.2 Ga Moodies Group, South Africa. See Noffke et al. (2006) for detailed description of the occurrence. (B) Variation in mat thickness in the tufted microbial mat of the Makgabeng Formation. (C) Mat fragment or mat chip from the Makgabeng Formation. Compare texture to A.

described below consisting of tufted microbial mat, biological soil crusts, and gas-escape structures bringing the total to six types of microbial mat-related structures that are now identified from the Makgabeng Formation.

5.1. Roll-up structures

5.1.1. Description

Roll-up features are restricted to interdune facies and the overlying dune plinth of the lower erg deposit and have not been recognized in the upper erg deposit (Bumby, 2000; Eriksson et al., 2000). We include mat chips and desiccated large mat fragments as described in Porada and Eriksson (2009) with the roll-up features (Fig. 6).

Roll-ups consist of silty mudstone laminations that are coiled through 2–3 revolutions, greater than 720° and less than 1060°

Table 1
Depositional facies.

Facies	Description	Interpretation
Lower Eolian Dune	Large-scale cross bed sets up to 3 m in thickness. Composed of wind-ripple strata and lesser grain flow. Rare 3rd order surfaces are present. 2nd order surfaces are trough shaped. Paleocurrents directed to the south-southwest.	Barchan and barchanoid dune deposits (Meinster and Tickell, 1975; Callaghan et al., 1991; Bumby, 2000; Eriksson et al., 2000; Simpson et al., 2002, 2004).
Upper Eolian Dune	Large-scale cross bed sets up to 8 m in thickness. Composed of wind-ripple strata and lesser grain flow. 3rd order surfaces are present and better developed than the lower facies. Near the upper contact massive sandstones are developed at the bases of some 3rd order surfaces. 2nd order surfaces are trough shaped near the top and more planer lower in the sections. Interdune deposits are very thin or absent. Paleocurrents directed to the south-southwest.	Barchan and barchanoid dune deposits (Meinster and Tickell, 1975; Callaghan et al., 1991; Bumby, 2000; Eriksson et al., 2000; Simpson et al., 2002, 2004).
Interdune	Lenticular traced up to minimum of 50 m. Maximum thickness to 80 cm. Sedimentary features present include wave-, combined flow- and current-ripples. Desiccation cracks are ubiquitous.	Deposits of wet interdune deposits (Bumby, 2000; Eriksson et al., 2000).
Playa	Lower playa up to 3.2 m thick and upper playa up to ~2.0 m thick. Mudstones present at base of with deep desiccation cracks developed in eastern outcroppings. Distinctive sedimentary features marking the former presence of efflorescent salt crusts are present including surface deformation features, such as deformed ripples and solution collapse structures represented by solution loading and growth faulting (Bumby, 2000; Simpson et al., 2004, 2012). Stacking of mudstone, sandstone, and interbedded mud/sandstone facies associations are present. Lower playa has all three facies associations. The upper playa is composed of the sandstone facies association (Simpson et al., 2012).	Stacking of facies associations reflects fluctuations in precipitation over longer time frames. In contrast, efflorescent crust features are consistent with shorter period (months or years) flooding followed by desiccation cycles (Simpson et al., 2004, 2012). The playa deposits indicate two periods of climatic amelioration during the Makgabeng erg history. (Simpson et al., 2004, 2012).
Fluvial	Composed of coarse sand size and pebbly coarse-grained sandstone near the contact with the Mogolokwena. Medium size trough cross beds predominate. A vertical sequence of horizontal stratification overlain by trough cross beds has been observed.	Ephemeral braided stream systems draining from the Limpopo Belt (Bumby, 2000).
Massive sandstones	Bases of massive sandstone are channelized or planar. Channel margins are low angle to vertical. May have vague horizontal stratification, ripped-up fragments of wind-ripple strata, rare dewatering structures, parting lineations, and capping adhesion structures. Sandstone bodies are lenticular and characteristically interbedded with low-angle to horizontal dune toesets. Lobate massive sandstone bodies vary from 5 cm to 6 m in thickness and from 3 m to possibly over 50 m in width. Some sandstone bodies onlap dune reactivation surfaces. Lower bound-aries of massive sandstone bodies change from channelized into lower planar-based down the dune foresets.	Massive sandstones were triggered by significant intense precipitation events and deposited from hyperconcentrated flows moving down the dune lee face. As hyperconcentrated flows migrated onto the dune plinth, rapid de-position produced lobate massive sandstone deposits with some flows maintaining turbulence onto the dune plinth. Massive sandstone bodies resting on reactivation surfaces are more likely a result of partial lee-face collapse (Bumby, 2000; Simpson et al., 2002).

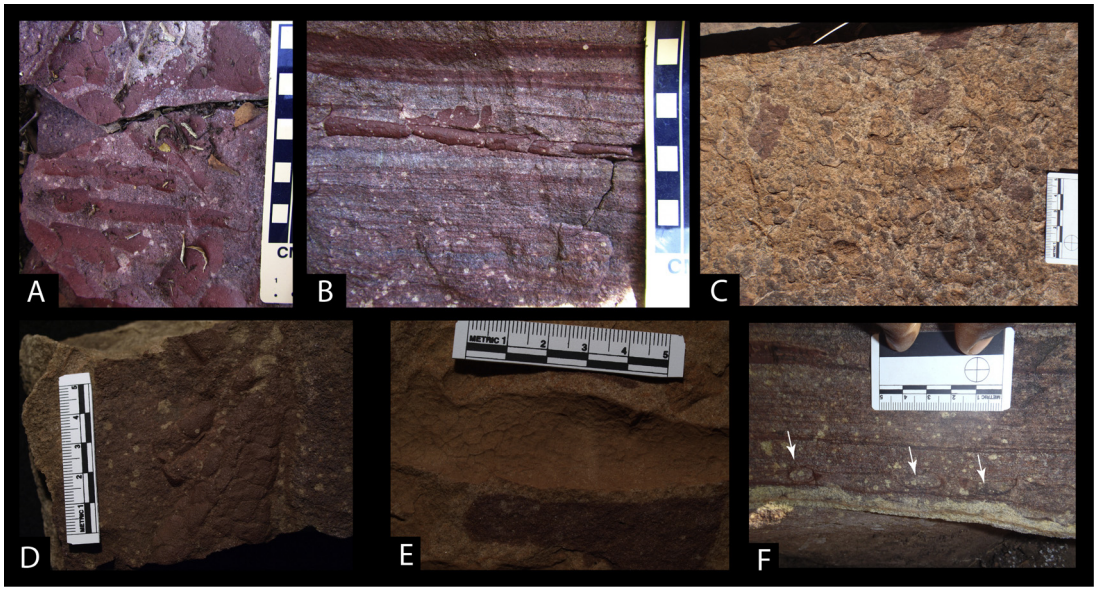

Fig. 6. Field photographs of mat fragments and roll-up features in the Makgabeng Formation. (A) Bedding plane view of mat fragments. These mat fragments are located at the transition from interdune deposits to overlying dune toe-set deposits. Scale is in cm. (B) Long axis view of roll-up features. These features are present in dune toe-set deposits above an extensive interdune deposit. Scale is in cm. (C) Bedding plane view of mat fragments. This mat fragment specimen is from interdune deposits. Scale is in cm. (D) Bedding plane view of large mat fragment. Note the sub-centimeter scale desiccation cracks. This specimen was found in float. Scale is in cm. (E) Bedding plane view of large mat fragment. This specimen was found in float. Note the sub-centimeter scale desiccation cracks. Scale is in cm. (F) Cross-section view of algal roll-up features. These features are present in dune toe-set deposits above an areally extensive interdune deposit. Arrows point out roll features. Scale is in cm.

of rotation (Eriksson et al., 2000). Laminations comprising roll-up features are commonly less than 1 mm thick (Fig. 6F). The features are circular to elliptical in cross-section. Roll-ups are preserved as elongate, cigar-shaped tubes up to 8 cm in length (Fig. 6B). Different scales of desiccation cracks typically define the upper surface of the laminations (Fig. 6D and E). Wrinkle structures are also present on these upper surfaces of the rolled up laminations. Mudstone chips are associated with the roll-up features (Fig. 6A–E). Chips vary in size from a few millimeters to 10 s of centimeters in length and width. Larger chips are curled and commonly display complex scales of desiccation cracks (Fig. 6D and E).

5.1.2. Interpretation

Since Eriksson et al.'s (2000) original interpretation of an algal origin, a series of experiments and observations in modern settings concerning the microbial mat origin of roll-ups have affirmed the assertion that the generation of these features requires the presence of microbial mats (Beraldi-Campesi and Garcia-Pichel, 2011; Bouougri and Porada, 2012). We have included the desiccated mud chips because they represent a spectrum of erosive energy and transport of mat-bound sediment after mat desiccation. Viable mechanisms that could have generated the roll-up features and desiccated mud chips in the Makgabeng interdune deposits include wind and water transport.

Detailed flume studies examining erosion of subaqueous mat-sediment binding products demonstrate that roll-up structures are linked with more mature, thicker microbial mats (Hagadorn and McDowell, 2012). Based on isolating specific parameters in these experiments,growth periods for thick mats are estimated at greater than 30 days and erosive velocities of more than ~30 cm/s but less than 40 cm/s. These are one set of possible conditions that can generate roll-up features. Additional observations of modern analogs on tidal flats and sabkhas produced a facies model that demonstrated the effect of windshear on the erodability of microbial mats (Bouougri and Porada, 2012). Wind shear across the mats generated a succession of features, from torn mats, folding and crumpling, flipped edges, and later wind-transported mat fragments. In this qualitative model, the development of roll-up features is restricted to the upper intertidal to the lower supratidal zone where mats and substrate were less saturated with water (Bouougri and Porada, 2012). Mat fragmentation developed in an upper supratidal-sabkha setting where mats are subjected to drier conditions.

The assignment of a biogenic origin to the roll-up features in the Makgabeng Formation is strongly supported by the experimental studies of Beraldi-Campesi and Garcia-Pichel (2011). The necessary presence of a mat adds pliability to mudstone allowing the muds to coil repeatedly, and this was tested by a series of experiments by Beraldi-Campesi and Garcia-Pichel (2011). These experiments confirmed that smectitic clays alone do not suffice to produce the concentric coiling found in continental microbial mats.

Based on the above, viable mechanisms for roll-up generation and fragmented mat transport in the Magkabeng Formation are probably wind and water movement. All of these experiments and observations affirm the original interpretation by Bumby (2000) and Eriksson et al. (2000, 2007). Porada and Eriksson (2009) suggest that the microbial mat roll-up features were induced by wind blowing across the Makgabeng Formation wet interdune areas and that the mats were coherent enough to survive transport onto the toes of the dune plinths. Higher wind velocities and longer distances of transport likely caused fragmentation of the microbial mats observed in Makgabeng Formation.

5.2. Sand cracks

5.2.1. Description

A spectrum of isolated to interconnected sand cracks occurs in the Makgabeng Formation (Figs. 7 and 8; Eriksson et al., 2007; Porada and Eriksson, 2009). Original reports from the area highlighted the occurrence of sand cracks in the interdune facies (Fig. 7). Recent fieldwork confirmed the occurrence of sand cracks in the interdune facies in the lower erg deposit and also recognized a wider distribution of the sand cracks into the lower portion of the playa facies. Sand cracks have not been identified from the upper erg strata.

Cracks are isolated and spindle shaped or connected in continuous crack systems displaying classic crack geometries, triple junctions and spindle forms (Figs. 7 and 8). Cracks are best developed on asymmetrically rippled bedforms preserved on bed tops and extend parallel to both the crests and troughs of bedforms (Fig. 7A). In some layers, cracks are restricted to the crests of bedforms. Junctions of

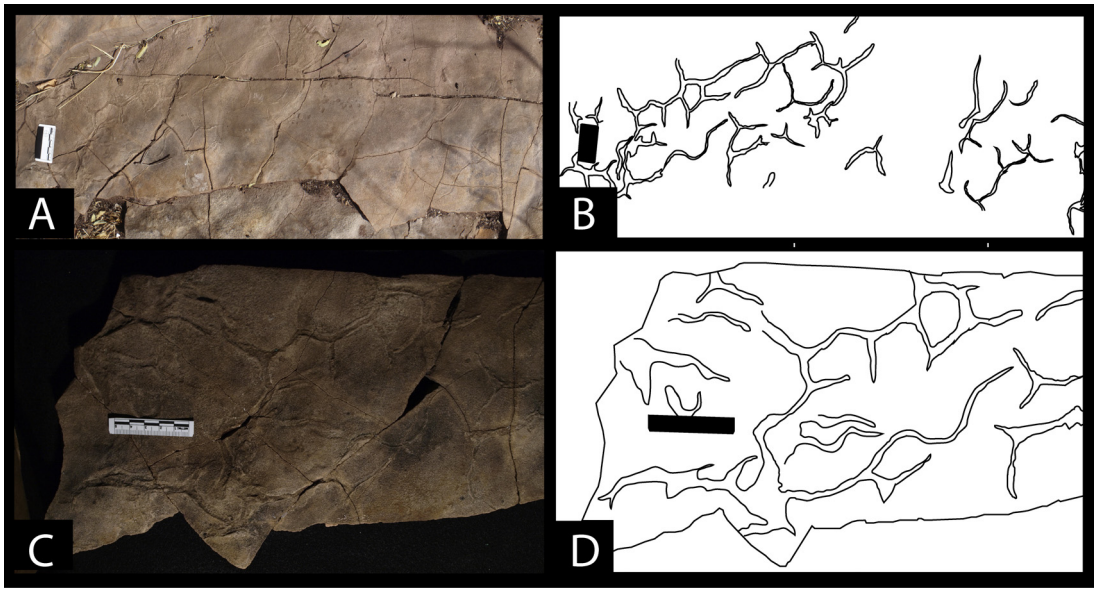

Fig. 7. Photographs of sand cracks. (A) Photomosaic of sand cracks in interdune deposit. Asymmetrical ripples cover the bedding plane. Scale card is 6 cm in length. Outlined block is slab in C. (B) Line drawing of crack system in A. (C) Slab photograph of sand cracks. Note the curving nature of the cracks and elevated crack rims. (D) Line drawing of crack system in C.

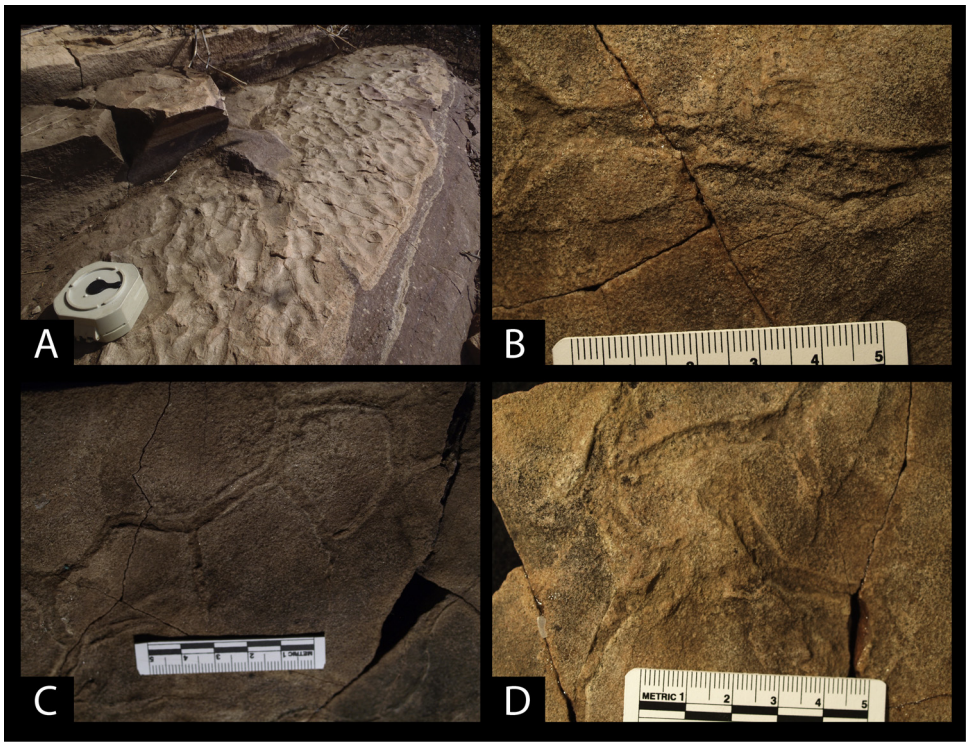

Fig. 8. Photographs of sand cracks. (A) Oblique field photograph of sand cracks with the crack system following the crest line of asymmetrical ripples. Brunton compass is 7 cm. (B) Two parallel crack systems. (C) Elevated crack rims. (D) Intersection of two trilete-shaped desiccation cracks. Note the complexity of the rim margins. Scale in B–D is in cm.

cracks are either sharply angled or sinuous (Fig. 8B and C). Margins of isolated cracks are sharp and some are slightly raised in elevation (Fig. 8C and D). Complex wrinkle features at the crack margins occur in completely connected crack systems (Fig. 8C), and graben-like features are present in thin section (Fig. 8B). Where developed independently, some cracks run parallel to each other (Fig. 8B). Atypical triple junction intersections are also present (Fig. 8D). On bedding planes, straight cracks are associated with and crosscut the sinuous cracks. The observed bedding surface with complex cracks also displays mm-scale irregular, rough, crinkled textures near the cracks.

In thin sections, up to three inferred mat layers are recognizable and are separated by, at most, 1 cm (Fig. 8). The spacing between observed mats in these cases decreases vertically (Fig. 9). Interpreted mat layers are nearly continuous across the thin section and composed of a series of discontinuous overlapping filaments. Margins of the cracks are "thickened" relative to the more distal areas, away from the crack. Soft sediment faults crosscut the sediment and mat layers (Fig. 9A). In thin section, soft-sediment fluidization is localized in the graben of one isolated crack system (Fig. 9B).

5.2.2. Interpretation

Silts and sands lack cohesion to form cracks and therefore muds or microbial mats are required to drive the cracking process (Schieber, 1998; Eriksson et al., 2007; Porada and Eriksson, 2009; Tang et al., 2012). Thin section work here demonstrates the presence of preserved mat features, affirming the microbial mechanism proposed by Eriksson et al. (2007) and Porada and Eriksson (2009) for the Makgabeng sand cracks.

Variation in the width and height of the sand cracks may reflect uneven mat thickness (Noffke et al., 2001; Bose and Chafetz, 2009). Sand cracks with more sinuous shape often are developed in troughs between ripples (Plüger, 1999; Eriksson et al., 2007) where the mats are thicker and, concomitantly, cracks are less well developed on the crests. The Makgabeng Formation cracks exhibit no preferential development in either crests or troughs, likely indicating a probable uniformly thick mat.

In the specific case of the Makgabeng Formation, inferred multiple mat horizons induced complex microstructural solutions to the tensional forces caused by mat desiccation (Fig. 8). The elasticity of the mat is reflected in the thickening of the sedimentary

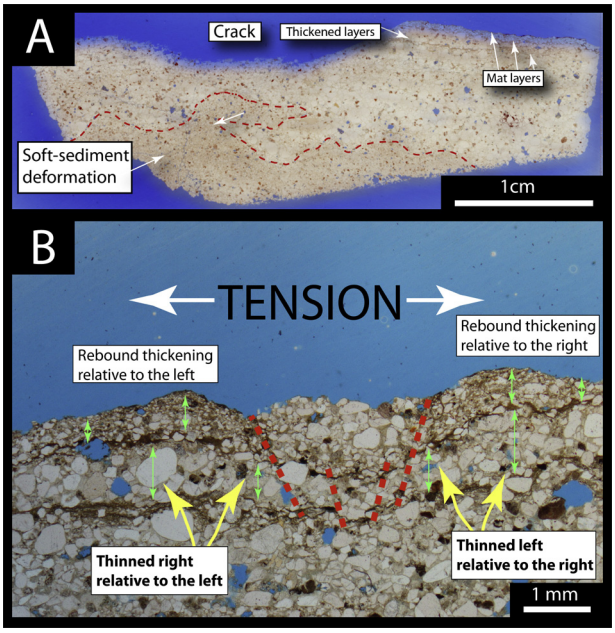

Fig. 9. Thin section photomicrographs of sand cracks. (A) Scan of thin section. Note the soft-sediment deformation in the graben area of the crack and thickening of sediment layering adjacent to the rupture zone. (B) Photomicrograph through desiccation feature. Scale bar is 0.5 mm. Nichols are parallel.

layering along the mat margin, from elastic "snap back" of the mat. The relatively rapid pull back of the sediment layer produced unloading over the graben and increased loading along the crack margin. If the bed was water saturated, the changes in load then induced fluidization in the central graben area with the lower confining pressure (cf. Lowe, 1975; Owen, 1996, 1997). If beds were not water saturated then the internal deformation style was brittle in character.

5.3. Wrinkle structures

5.3.1. Description

Wrinkle structures are restricted to interdune deposits and have been identified from only a single bed (Fig. 10). The upper bedding surface exposes ridges and swales that are crudely parallel with a mean spacing of approximately 5 mm and with a maximum of ~15 mm. Other ridge trends are oblique and form very crude reticulate patterns. A larger mound-like structure shows ridges radiating from the mound-peak (Fig. 10C).

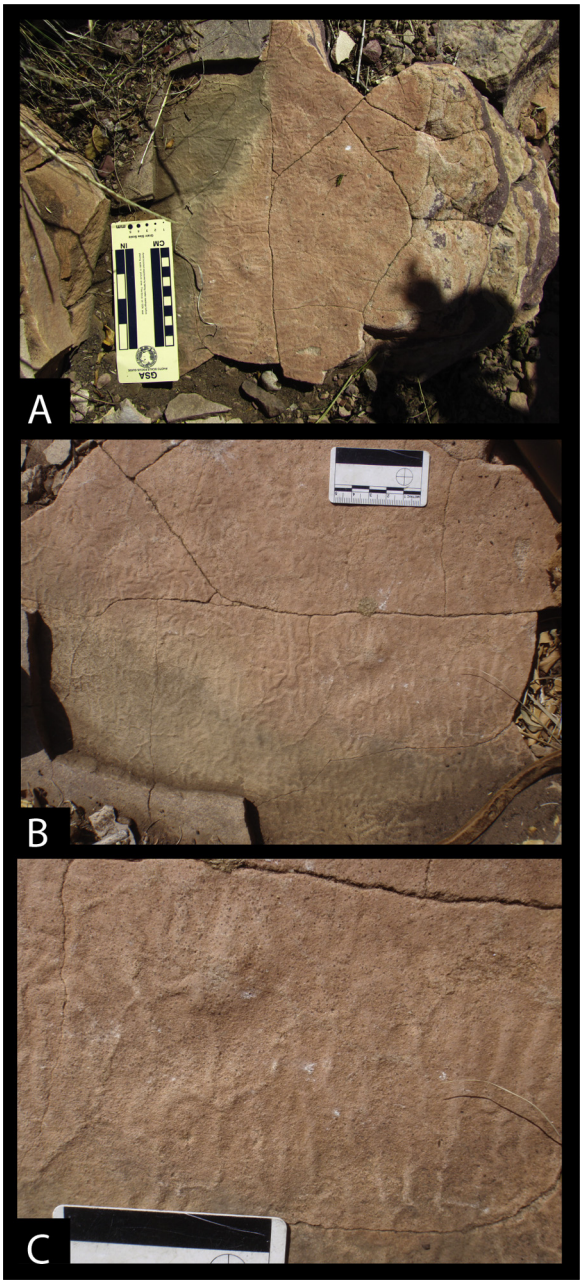

Fig. 10. Field photographs of the wrinkled mats on bedding planes. (A) Outcropping of wrinkled mats in interdune deposit. Scale is in cm. (B) Enlargement showing complex, wrinkle morphology. Scale is in cm. (C) Wrinkle mat close up. In top portion is an elevated mound with radiating wrinkles. Scale is 5 cm.

In thin section, mat features are preserved above an irregular topography consisting of a larger sand-size grain mantle (Fig. 11). The mat features are developed in siltstone and are reflected as irregular, discontinuous laminations at the bottom of the siltstone and more continuous mats at the top of the bed (Fig. 11A and B). Internally the siltstone bed laminations deflect and drape the larger grains at the interface with the underlying bed. The lamination inclination decreases from vertical to near horizontal, but they display undulations over a larger scale. The core of the bed comprises graded siltstone (Fig. 11A and B). Organic fragments define laminations in the graded bed and increase in abundance vertically. At the top of the bed, organic laminations are of higher density and contain floating silt grains.

5.3.2. Interpretation

Wrinkle structures are formed and are preserved in sediment beneath microbial mats (Hagadorn and Bottjer, 1997, 1999; Porada and Bouougri, 2007a,b). They are found in a diverse paleogeographic range, from deep marine to a variety of continental environments (Hagadorn and Bottjer, 1997, 1999; Noffke, 2000; Porada and Bouougri, 2007a,b; Mata and Bottjer, 2009). A variety of mechanisms have been proposed for the genesis of mat wrinkling including: (1) tractional shear across the mat surface (Hagadorn and Bottjer, 1997; Bouougri and Porada, 2002), (2) gas expulsion (Plüger, 1999), (3) loading (Noffke et al., 2002), and (4) primary growth topography (Schieber, 2004). Proposed producers of wrinkle structures include cyanobacteria, sulfur-oxidizing bacteria, or green sulfur bacteria (Mata and Bottjer, 2009). Motility of cyanobacteria generates unidirectional sliding and colliding of filaments that translate into a more organized reticulate pattern in the larger mat structure (Shepard and Sumner, 2010).

Thin sections from this study demonstrate that initially mat and sediment draped the underlying bed topography that consisted of coarse grains of sand. These coarse grains of sand at the abrupt transition probably represent a deflation lag developed on the underlying sandstone bed (cf., Clemmenson and Tirsgaard, 1990). These deflation lags would develop with the water table below the sediment–air surface, followed by an increase in precipitation that raised the water table, thus permitting the development of the overlying microbial mat at the sediment–water interface (e.g. Loope, 1985; Fryberger et al., 1988; Langford and Chan, 1989; Fryberger, 1990). Silt-sized grains were delivered to the interdune area through suspension settling (dust). Silt is commonly laid down in interdune settings (Ahlbrandt, 1979; Fryberger et al., 1983; Simpson and Loope, 1985). This dust consisted predominantly of quartz grains and probable fragments of microbial mats. Mat fragments remain coherent even through extensive wind transport (Bouougri and Porada, 2012). After filling and stabilization of the initial relief the microbial mat leveled out the topography (Fig. 9; see Noffke, 2010). The best-developed mat occurs at the top of the bed reflecting limited detrital input and signaling the end of the sedimentation unit.

5.4. Tufted microbial mat

5.4.1. Description

Tufted microbial mat features are restricted to interdune deposits. The features are found on top of a ~1 cm-thick fine-grained sandstone bed. The sole of the bed possesses casts of the cracked sandstone bed below. The bed surface is rough and displays an uneven texture that is randomly punctuated by 2 mm-tall

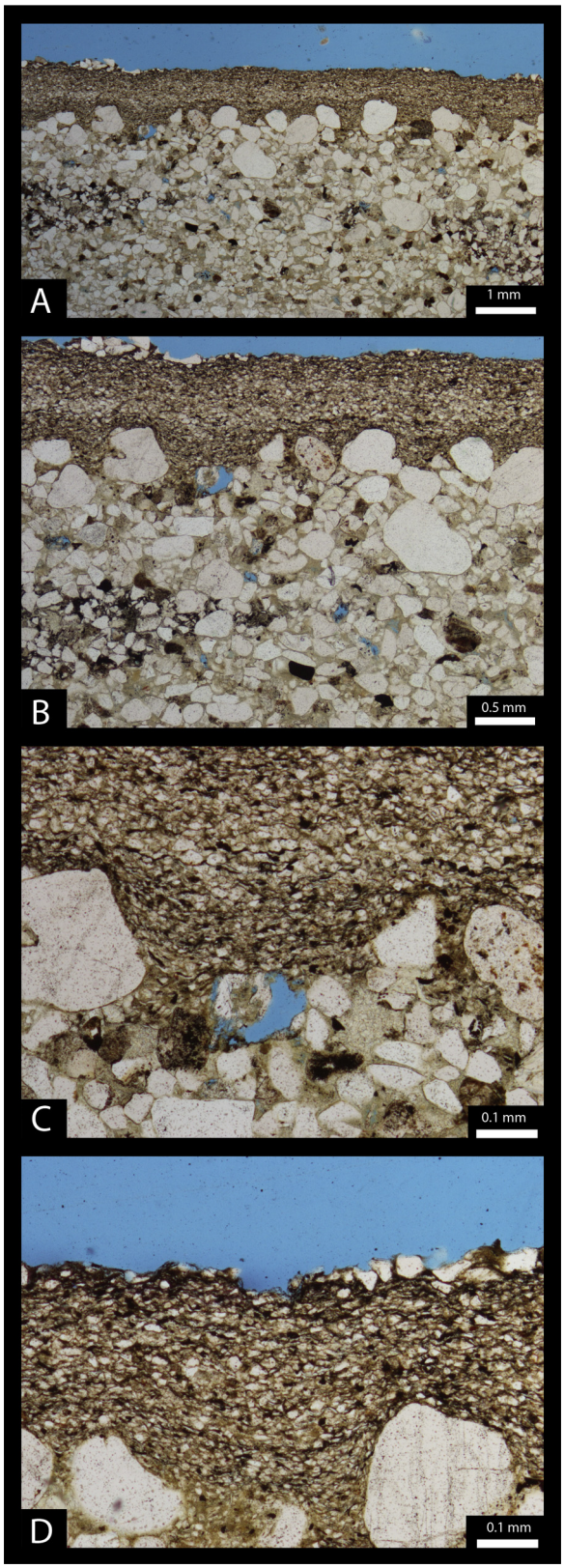

Fig. 11. Thin section photomicrographs of wrinkled mats. All are photographed in plane light. (A) Thin section of wrinkle features. Note the large grains armor the sandstone interval. (B) Variation of texture across the siltstone interval. (C) Change in orientation around sand gains. (D) Best mat development at the top of the photograph.

vertical bump-like structures (Fig. 12). Bumps display no preferred orientation but some are more elongate rather than round (Fig. 12).

In thin section, the centimeter-thick bed displays fine sandstone at the base replaced vertically by medium-grained sandstone (Fig. 13A). The top of the bed consists of fine-grained sandstone again (Fig. 13A). The mat developed on the bumpy features contained floating grains in silt to very fine-grained sand size. Microtopography consists of millimeter-scale bumps cored by fine-grained sandstone (Fig. 13A). Variation in the thickness of the inferred mat features is linked to the microtopography (Fig. 13A and B). Microtopographic highs are characterized by thinner mat drapes or even their absence, whereas microtopographic lows are associated with thicker inferred mat features.

5.4.2. Interpretation

The interpretation of this mat type is problematic as it may represent either inherited sedimentary topography filled by a mat, or a tufted microbial mat. Tufted-mat features are recognized and described from modern marine strandline settings where tufts are attributed to polarity changes in the growing filamentous cyanobacteria. The result is a condensed fibrillar meshwork that is elevated several millimeters above the basal mat (Gerdes et al., 2000; Noffke, 2010). Bose and Chafetz (2009) report high tufts of mats at the intersection of microbial bulges in their reticulate mat features. These types of mats form in the upper intertidal zone with little moisture content except that which is derived from very high water levels or from precipitation (Bose and Chafetz, 2009). In addition they have been recognized in Archean lacustrine deposits (Flannery and Walter, 2012). The recognition of tufted mat features at either the microscopic or macroscopic level provide unambiguous evidence for the presence of MISS (Noffke, 2009, 2010). In the Makgabeng Formation this feature, if reflecting a tufted mat, potentially provides unambiguous evidence for the presence of microbial mats.

5.5. Biological soil crusts

5.5.1. Description

Biological soil crust (BSC) features are located along a bedding plane at the transition from the lower erg into the lower playa (Figs. 3C and 14). This stratal boundary between the two facies displays undulating relief of up to 50 cm (Fig. 3C). The features are preserved on the highest and least eroded points along the stratal boundary. The BSCs consist of preserved patches of poorly sorted, fine-grained sandstone with 1 cm-wide diffuse desiccation features. The cracks are best developed on the surface of the highest elevation (Fig. 14A and B). At the edges, the desiccation features are less deep. Individual polygon surfaces are irregular in shape and possess a bumpy, irregular surface between cracks. These cracks are not as sharp or distinctively shaped compared to the cracked sandstone features. Due to the nature of the exposure and their rarity, these features were not sampled for thin section analysis. No mat-like features were apparent in 10x hand lens analysis.

5.5.2. Interpretation

In modern semi-arid and arid settings, BSCs are well developed and broadly defined as complex symbioses of eubacteria, cyanobacteria, algae, lichens, bryophytes, and fungi that create coherent crusts within the upper few centimeters of a soil profile (West, 1990; Belnap and Gillette, 1998; Belnap et al., 2001). BSCs stabilize land surfaces through the binding action of the microflora, which also increases the preservation potential of BSCs to enter the rock record (Campbell, 1979; Belnap et al., 2001; Prave, 2002; Retallack, 2008; Malenda et al., 2012). Most studies of BSCs or

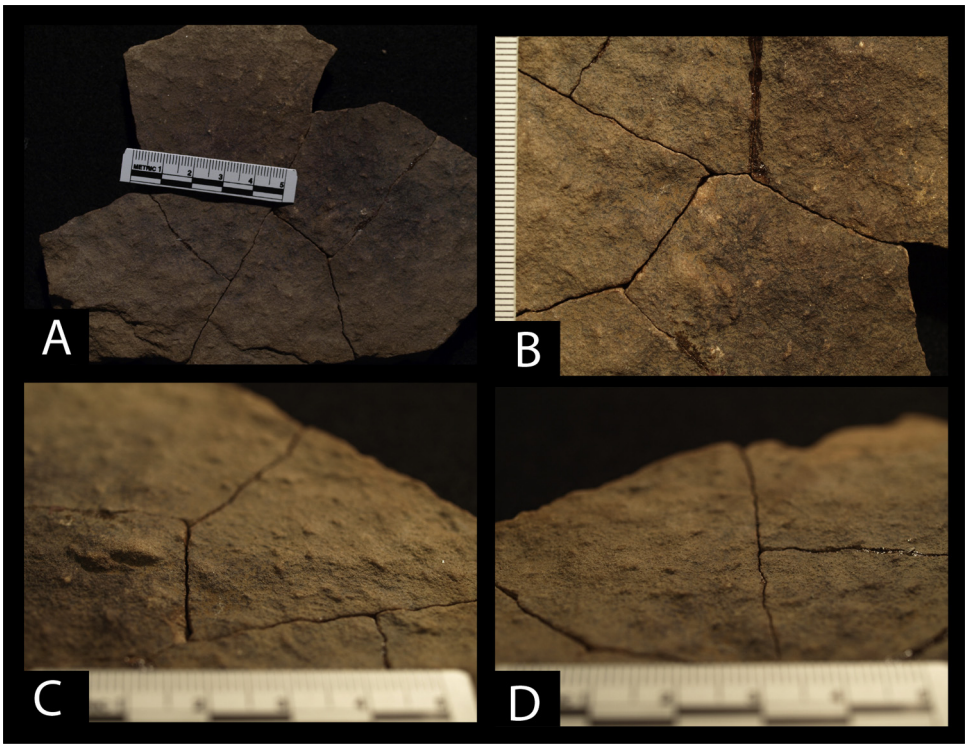

Fig. 12. Slab photographs of the tufted microbial mat. Scale in all photographs is in mm.

continental microbial mats commonly fail to identify preserved organic matter in the BSC because of the porous nature of the sandstone (Prave, 2002; Simpson et al., 2010) with the exception of Sheldon (2012). The preservation of the upper few centimeters of a weakly developed soil profile could occur along erosional microtopographic highs. This was likely the case for these BSCs that occur along highs on the stratal boundary between the lower dune and playa facies. The early flooding stage of the playa was a rapid expansion phase (Simpson et al., 2004, 2012) that potentially eroded into the underlying dune deposits, breaching the once more extensive and well-developed BSC surface.

Caution must be used so as not to confuse BSC morphology with physical sedimentary structures, such as adhesion features, adhesion warts, and evaporitic crusts (Kocurek and Fielder, 1982; Olsen et al., 1989; Chakraborty and Chaudhuri, 1993; Simpson and Eriksson, 1993; Smoot and Castens-Seidell, 1994). Descriptions of vertical cross-sections through vertically accreting BSCs are rare (Simpson et al., 2010; Malenda et al., 2012). Based on the surface morphology of modern biological soil crusts, the Makgabeng Formation features are best interpreted as preserved biological soil crusts (Belnap and Gillette, 1998; Belnap et al., 2001). Malenda et al. (2012) document similar morphological features from BSCs in Utah. The Utah BSCs display diffuse desiccation cracks and bumpy surfaces on the polygons (Fig. 13C). In addition, Malenda et al.'s (2012) features are characteristic of the destructive phase of biological soil crusts. Malenda et al. (2012) illustrate some of the three-dimensional subsurface pedogenic features associated with the Colorado plateau biological soil crusts in Utah. Poor sorting may be a useful tool in supporting a biological soil crust origin. The sticky secretions (extrapolymeric substance or EPS) of the cyanobacteria in biological soil crusts bind atmospheric dust (silt and clay size material), allowing for unsorted sediment compositions as a potential indicator of the presence of a BSC (Zaady and Offer, 2010; Simpson et al., 2010; Malenda et al., 2012). In an environment where sediment is very well sorted by physical processes, unsorted material can provide evidence for BSCs (Zaady and Offer, 2010; Simpson et al., 2010). The Makgabeng Formation BSCs display poor sorting, consistent with this observation.

Flora and fauna in BSCs are limited in their ability to grow vertically to capture light (Belnap et al., 2003). More efficient light gathering plants therefore limit the BSC distribution (Belnap et al., 2003). Therefore, before the advent of land plants BSCs should have been distributed more widely and would have been found in more diverse environments than in modern times (Campbell, 1979; Prave, 2002; Retallack, 2008).

BSC microbial diversity and comparative abundances of microbial components can be inferred from their physical morphologies (Belnap et al., 2001, 2003), including smooth, rugose, pinnacled, and rolling versions (Johansen, 1993; Eldridge and Greene, 1994; Belnap et al., 2001). For example, crusts dominated by cyanobacteria with little or no lichens and mosses form smooth biological soil crusts, while a crust dominated by cyanobacteria and lichens produces a pinnacled morphology (Belnap et al., 2001; Belnap, 2003). The Makgabeng BSCs are closer in appearance to the smooth morphology, and hence were probably composed of a community characterized by cyanobacteria.

5.6. Gas-escape features

5.6.1. Description

Gas-escape features are best developed on a single bedding plane surface in fine-grained sandstone near the base of an interdune deposit (Fig. 15). Sparse inferred gas-escape structures are present along a sand-cracked bed-top at the base of the playa deposit. The bedding plane displays irregular topographic depressions and highs of less than 3 cm; the inferred gas-escape features are crude circular to oval-shaped depressions (Fig. 15D). Concentric laminations surround some of the depressions and are parallel in orientation with the edge of the depression (Fig. 15C).

These features are distributed across the bedding surface either as single or tightly clustered circular- to oval-shapes (Fig. 15D).

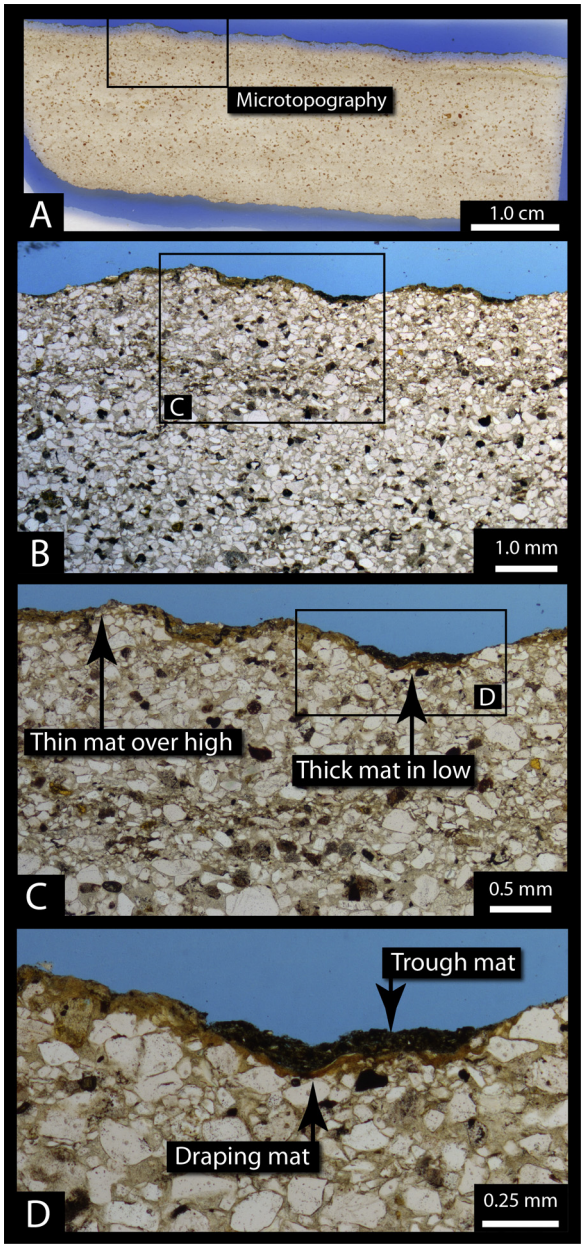

Fig. 13. Tufted microbial mat. All photomicrographs are taken under plane light. (A) Scan of thin section of tufted mat. Thin section is ~4.0 cm in width. Note box showing the location of B. (B) Enlargement of thin section displaying thickness variation across the tufted mat surface. The preserved mat is thicker in the lows and thinner in the highs. Scale bar is 1 mm. Boxes show the positions of figures C and D. (C) Thick mat with contortions that overlie more planar mat surface. Scale bar is 0.5 mm. (D) Thicker mat composed of two different textured features. Scale bar is 0.25 mm.

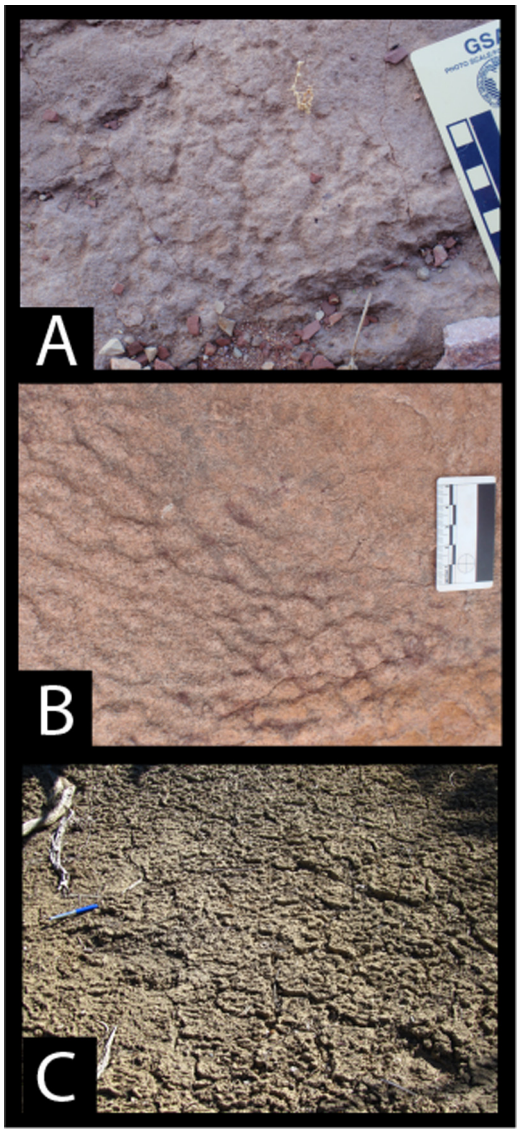

Fig. 14. Field photographs of modern and ancient biological soil crusts. (A) Preserved biological soil crust at the boundary between the dune and playa deposits in the Makgabeng Formation. Note the polygonal desiccation features and the microtopography on the polygonal features. Scale is in centimeters. (B) Preserved biological soil crust at the boundary between the dune and playa deposits in the Makgabeng Formation. Note the lateral change in morphology of the desiccation features and the reduction in development to the left of the photograph. Scale is in centimeters. (C) Modern biological soil crust located at Grand Staircase Escalante National Monument, Utah, USA. This biological soil crust shows faint, weakly developed desiccation features with microtopographic relief between the desiccation features.

At the center of some of the oval features are elevated craters; some depressions have these oval laminations at their margins. Laminations are parallel to some depressions and faint, parallel linear grooves crosscut the bed surface in the interdune setting.

5.6.2. Interpretation

These bed-top features record internal deformation structures below a microbial matted surface probably related to gas dome generation (Noffke et al., 1996, 2008). The mat layer was eroded exposing shallow degassing structures associated with the decaying of microbial mats (cf., Reineck et al., 1990; Dornbos et al., 2007). Based on the presence of faint linear grooves, two dimensional ripple bedforms capping the bed were eroded with only the lowest portion of the troughs preserved. A scour event reworked the bed-top exposing the underlying internal structures beneath the mats.

Microbial-related gases are generated by both mat growth and mat decay processes (Stal, 1994). Noffke et al. (1996, 2008) analyzed interstitial gas and identified CH_4, CO, CO_2, H_2, H_2S and other gases. Additional potential sources of gas include decomposition of organic matter, gas diffusion, decreased diffusion caused by cohesive organic laminations, and compaction (Gerdes et al., 2000). These gases can be vented to the surface and may be recorded as singular to clustered oval features that represent the original position of the conduits. Low depressions with concentric laminations reflect potential collapse of the underlying layers due to decay of the microbial mats (Noffke, 2010).

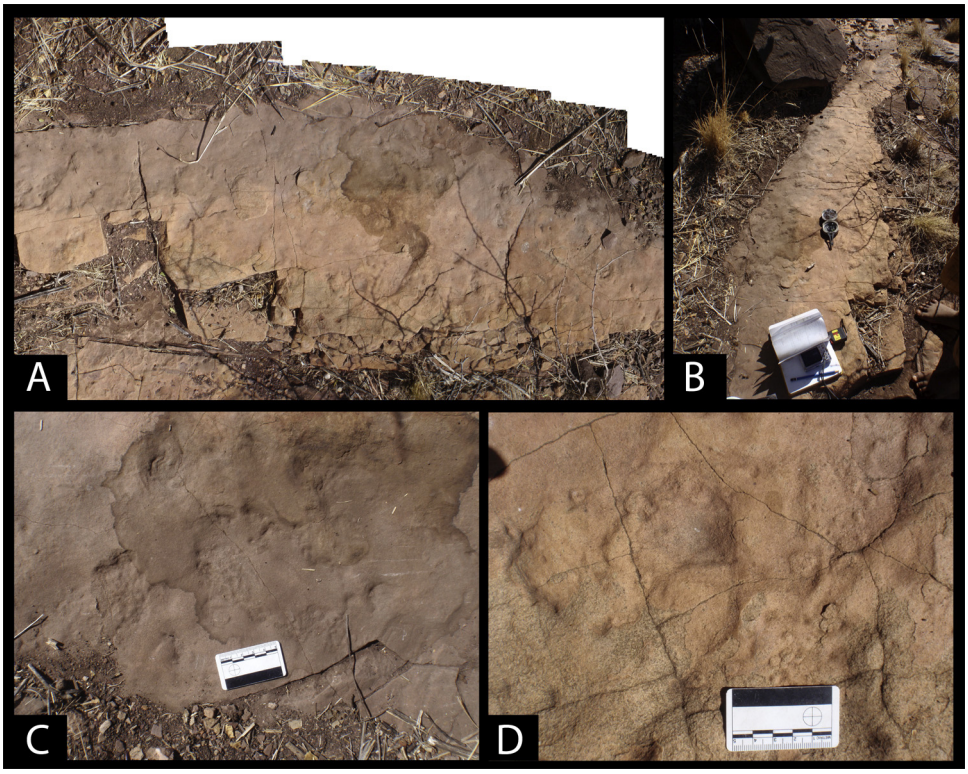

Fig. 15. Field photographs of gas-escape features preserved in an interdune deposit. (A) Vertical photomosaic of bedding plane surface in interdune deposits. (B) Oblique-angle photograph of the bedding plane. (C) Close up of gas-escape structures with internal laminations exposed on the bedding plane. Scale is in cm. (D) Concentric gas-escape features. Scale in cm.

6. Discussion

The number of MISS features recognized from Precambrian continental settings recently has increased in abundance (Callow et al., 2011; Sheldon, 2012). Here the catalog of known microbial mat-related sedimentary features is increased from one of the oldest paleo-desert deposits globally (Fig. 16; the ~2.0 Ga Makgabeng Formation, Waterberg Group, South Africa).

The inferred BSCs, based on comparison with modern examples in the literature, are compatible with semi-arid to arid settings and reflect complex symbiotic organic communities that form coherent crusts in the uppermost parts of soil profiles (West, 1990; Belnap and Gillette, 1998; Belnap et al., 2001). BSC preservation on the stratal boundary in the Makgabeng Formation suggest a destructive interpretation, due to rapid initial playa expansion that breached an originally extensive BCS surface and eroded down into the underlying dune deposits (Section 5.5).

The MISS and BSC features documented from the Makgabeng Formation together indicate preponderance of mat destruction, but with mat growth and metabolism, biostabilization also unequivocally supported. This expanded catalog of proxies signals the presence of a robust and thriving Paleoproterozoic continental microbial ecosystem, approximately 200 million year after the Great Oxidation Event (GOE; cf., Holland, 2006). The recognition of these features from diverse depositional settings (Fig. 16) in the Makgabeng Formation also implies that the ability of microbes to survive desiccation and long-distance wind transport into dryland paleoenvironments had evolved by 2.0 Ga (as also postulated by Eriksson et al., 2000). Recent geochemical proxies using complex organic molecules that have evolved to protect

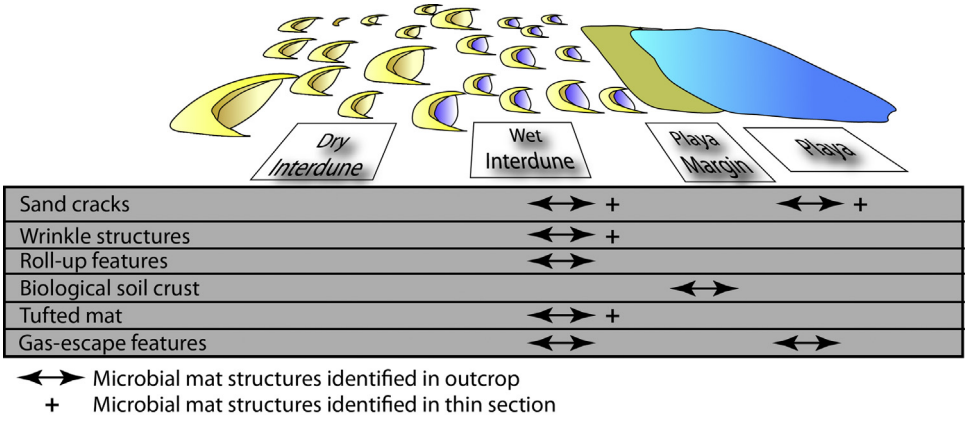

Fig. 16. Paleoenvironmental distribution of microbial mat features in the Makgabeng Formation.

against microorganism desiccation argue that terrestrial life probably gained a foothold in extreme environments, such as playas or saline pans (see Finkelstein et al., 2010) and our observations from the Makgabeng Formation are consistent with this hypothesis.

The GOE at ~2.3 Ga marks one of the most significant transitions in the history of the Earth (Holland, 2002). Although a complex and multi-faceted subject, the accumulation of atmospheric oxygen (i.e. the GOE) was strongly influenced by the switch from reducing to oxidizing volcanic gases that preceded the transition (Kump et al., 2001; Holland, 2002; Eriksson et al., 2013). The transition to an oxidizing atmosphere commonly has been linked to the evolutionary development of cyanobacteria around this time frame (e.g., Ohmoto, 2004 and references therein). Buick (2008) argues that photosynthetic oxygen started before of onset of the GOE.

The recognition of Archean continental microbial life is based mainly on paleosol proxies and lacustrine stromatolites. Paleosol evidence is commonly predicated on major element distribution in the inferred soil profile, preserved organic filaments and analogy with modern soils. Based on the mobility of phosphorus in the paleosol profile, Driese et al. (2011) argue for the presence of a significant terrestrial microbial biomass at ~2.7 Ga that aided in the weathering of the Saganaga Tonalite along an unconformity surface beneath the Ogishkemuncie Congolmerate in Minnesota, USA. Prasad and Roscoe (1996) described a vertical change in chemistry from a weathering profile dated at ca. 2.45–2.22 Ga, from lower and upper sub-Huronian paleosols. Gutzmer and Beukes (1998) argue via analogy that ~2.0–2.2 Ga laterites show that terrestrial life was present along with an oxygenated atmosphere. Carbon filaments have been identified petrographically in auriferous conglomerates of the Neoarchean Witwatersrand gold deposits that may have been wind transported across the placer surface (Mossman et al., 2008).

Lacustrine stromatolites have been cited as the earliest proxy for terrestrial life (Buick, 1980, 1992; Awramik and Buchheim, 2009). The assignment of a lacustrine setting is often problematic because of the absence of facies that are solely indicative of such an environment. This conundrum also relates to stromatolites in the Archean Fortescue Group (Australia) with one group of workers arguing the facies reflect a marine setting (Packer, 1990; Thorne and Trendall, 2001; Sakurai et al., 2005) whereas others interpret the same facies as lacustrine (Kriewaldt and Ryan, 1967; Walter, 1984; Buick, 1992; Blake et al., 2004; Walter and Allwood, 2005; Bolhar and Van Kranendonk, 2007; Awramik and Buchheim, 2009). Stromatolites have been recognized in distal shallow lacustrine systems of the Omdraaivlei Formation, Sodium Group of the 2.7 Ga Ventersdorp Supergroup (Kaapvaal craton; Altermann and Lenhardt, 2012).

BSCs display specific textural features that permit their recognition in the rock record, but a lower probability of preservation limits their usefulness. Only four examples of BSCs have been reported from the rock record: (1) 1.2 Ga (Prave, 2002), (2) 1.1 Ga (Sheldon, 2012), (3) Cambrian (Retallack, 2008), and (4) Cretaceous (Simpson et al., 2010). The inferred BSCs in the Makgabeng Formation predate the oldest recognized example by nearly 800 million years.

What also distinguishes the Makgabeng evidence for a robust ecosystem at ca. 2.0 Ga, is that the microbial features apparently survived and indeed thrived within a paleo-desert setting, subject to significant paleoclimatic changes. The occurrence of two inferred erg deposits separated by an extensive playa deposit (Figs. 3A and 4 and Table 1; Bumby, 2000; Heness et al., 2012), and the vertical increase in wet interdune deposits toward the lower erg-playa contact support climatic variability and transition (Figs. 3B and 4; Eriksson et al., 2000; Heness et al., 2012). The transition itself is abrupt and marked by the interpreted BSC features. While interdune deposits in the upper erg are very thin (Fig. 3D), once again near the top of this inferred paleo-dune succession, playa and ephemeral fluvial beds increase, reflecting enhanced precipitation (Fig. 4; Bumby, 2000; Heness et al., 2012). Close to the upper contact of the Makgabeng Formation with the succeeding fluvial Mogalakwena Formation, massive sandstones related to catastrophic deluges become more prevalent, again supporting paleoclimatic changes, in this case amelioration that signaled the end of upper erg development (Fig. 4; Bumby, 2000; Simpson et al., 2004; Heness et al., 2012).

7. Summary

- Three new biogenic features (biological soil crusts [BSC], tufted microbial mat, and gas escape features) are added to the existing catalog of roll-up structures (and associated mat chips), sand cracks, and wrinkled features within the ca. 2.0 Ga Makgabeng Formation of South Africa.
- The microbially related structures are observed within interdune deposits within the lower erg, playa margin, and playa facies.
- Interpretations of both MISS and BSC features support microbial mat growth, metabolism and destruction, with the latter apparently having been more prevalent.
- The inferred BSCs are approximately 800 Myr older than previously described in literature.
- Our data and interpretations imply that the microbes were able to survive desiccation and transport in dryland environments, and that a thriving microbial community flourished within a paleo-desert within about 200 Myr of the Great Oxidation Event.
- MISS and BSC proxies thus allow paleoclimatic interpretations and enhance paleoenvironmental models, in a way analogous to body fossils and ichnological features.

Acknowledgements

This research was supported by the Kutztown University Undergraduate Research Committee, Kutztown University Research Committee, Kutztown University Foundation, Kumba-Exxaro, South Africa, the National Research Foundation of South Africa, and the University of Pretoria, South Africa. The comments of two anonymous reviewers improved the quality of the manuscript.

References

Ahlbrandt, T.S., 1979. Textural parameters of eolian deposits. In: McKee, E.D. (Ed.), A Study of Global Eolian Deposits. United States Geological Survey Professional Paper 1052, pp. 21–52.

Altermann, W., Lenhardt, N., 2012. The volcano-sedimentary succession of the Archean Sodium Group, VentersdorpSupergroup. South Africa: Volcanology, sedimentology and geochemistry. Precambrian Research 214–215, 60–81.

Awramik, S.M., Buchheim, H.P., 2009. A giant, Late Archean lake system: The Meentheena Member (Tumbiana Formation; Fortescue Group). Western Australia. Precambrian Research 174, 215–240.

Battistuzzi, F.U., Feijo, A., Blair Hedges, S., 2004. A genomic timescale of prokaryote evolution: insights into the origin of methanogenesis, phototrophy, and colonization of land. BMC Evolutionary Biology 4–44, 1–14.

Belnap, J., 2003. The world at your feet: desert biological soil crusts. Frontiers in Ecology and Environment 1, 181–189.

Belnap, J., Büdel, B., Lange, O.L., 2003. Biological soil crusts: characteristics and distribution. In: Belnap, J., Lange, O.L. (Eds.), Biological Soil Crusts: Structure, Function and management. Ecological Studies 150. Springer, New York, pp. 3–30.

Belnap, J., Gillette, D.A., 1998. Vulnerability of desert biological soil crusts to wind erosion: the influences of crust development, soil texture, and disturbance. Journal of Arid Environments 39, 133–142.

Belnap, J., Kaltenecker, J.H., Rosentreter, R., Williams, J., Leonard, S., Eldridge, D., 2001. Biological soil crusts: ecology and management. United States Department of Interior Technical Reference 1730–1732, 110.

Beraldi-Campesi, H., Garcia-Pichel, F., 2011. The biogenicity of modern terrestrial roll-up structures and its significance for ancient life. Geobiology 9, 10–23.

Beraldi-Campesi, H., Hartnett, H.E., Anbar, A., Gordon, G.W., Garcia-Pichel, F., 2009. Effect of biological soil crusts on soil elementalconcentrations: implications for biogeochemistry and astraceablebiosignatures of ancient life on land. Geobiology 7, 348–359.

Blake, T.S., Buick, R., Brown, S.J.A., Barley, M.E., 2004. Geochronology of a late Archean flood basalt province in the Pilbara Craton Australia: constraints on

basin evolution, volcanic and sedimentary accumulation, and continental drift rates. Precambrian Research 133, 143–173.
Bolhar, R., Van Kranendonk, M., 2007. A non-marine depositional setting for the northern Fortescue Group, Pilbara Craton, inferred from trace element geochemistry of stromatolitic carbonates. Precambrian Research 155, 229–250.
Bose, S., Chafetz, H.S., 2009. Topographic control on distribution of modern microbially induced sedimentary structures (MISS): A case study from Texas coast. Sedimentary Geology 213, 136–149.
Bouougri, E.H., Porada, H., 2002. Mat related sedimentary structures in the Neoproterozoicperitidal passive margin deposits of the West African Craton. Sedimentary Geology 153, 85–106.
Bouougri, E.H., Porada, H., 2012. Wind-induced mat deformation structures in recent tidal flats and sabkhas of SE-Tunisia and their significance for environmental interpretation of fossil structures. Sedimentary Geology 263–264, 56–66.
Buick, R., 1980. Stromatolite and ooid deposits within fluvial and lacustrine sediments of the Precambrian VentersdorpSupergroup of South Africa. Precambrian Research 12, 311–330.
Buick, R., 1992. The antiquity of oxygenic photosynthesis: Evidence from stromatolites in sulphate-deficient Archean lakes. Science 255, 74–77.
Buick, R., 2008. When did oxygenic photosynthesis evolve? Philosophical Transactions of the Royal Society B 363, 2731–2743.
Bumby, A.J., 2000. The geology of the Blouberg Formation, Waterberg and SoutpansbergGroups in the area of Blouberg mountain, Northern Province, South Africa. University of Pretoria, Pretoria, South Africa (PhD Dissertation), 331 p.
Bumby, A.J., Eriksson, P.G., Van Der Merwe, R., 2004. The early Proterozoic sedimentary record in the Blouberg area, Limpopo Province, South Africa; implications for the timing of the Limpopo orogenic event. Journal of African Earth Sciences 39, 123–131.
Bumby, A.J., Eriksson, P.G., Van Der Merwe, R., Brümmer, J.J., 2001. Shear-zone controlled basins in the Blouberg area, Northern Province, South Africa: syn- and post-tectonic sedimentation relating to ca. 2.0 Ga reactivation of the Limpopo Belt. African Earth Sciences 33, 445–461.
Callaghan, C.C., Eriksson, P.G., Snyman, C.P., 1991. The sedimentology of the Waterberg Group in the Transvaal South Africa, an overview. Journal of African Earth Sciences 13, 121–139.
Callow, R.H.T., Battison, L., Brasier, M.D., 2011. Diverse microbially induced sedimentary structures from 1 Ga lakes of the Diabaig Formation, Torridon Group, northwest Scotland. Sedimentary Geology 239, 117–128.
Campbell, S.E., 1979. Soil stabilization by prokaryotic desert crust: implications for Precambrian land biota. Origins of Life 9, 335–348.
Chakraborty, T., Chaudhuri, A.K., 1993. Fluvial-aeolian interactions in a Proterozoic alluvial plain: example from the Mancheral Quartzite, Sullavai Group, Pranhita-Godavari Valley, India. In: Pye, K. (Ed.), The Dynamics and Environmental Context of Aeolian Sedimentary Systems. Geological Society of London Special Publication 72, pp. 127–141.
Clemmenson, L.B., Tirsgaard, H., 1990. Sand-drift surfaces: a neglected type of bounding surface. Geology 18, 1142–1145.
Dorland, H.C., Beukes, N.J., Gutzmer, J., Evans, D.A.D., Armstrong, R.A., 2006. Precise SHRIMP U–Pb zircon age constraints on the lower Waterberg and Soutpansberg Groups, South Africa. South African Journal of Geology 109, 139–156.
Dornbos, S.Q., Noffke, N., Hagadorn, J.W., 2007. Mat-decay features. In: Schieber, J., Bose, P.K., Eriksson, P.G., Banerjee, S., Sarkar, A., Altermann, W., Catuneanu, O. (Eds.), Atlas of microbial mats features preserved within the siliciclastic rock record. Atlases in Geosciences 2,. Elsevier, New York, pp. 106–110.
Dott Jr., R.H., 2003. The importance of eolian abrasion in supermature quartz sandstones and the paradox of weathering on vegetation-free landscapes. Journal of Geology 111, 387–405.
Driese, S.G., Jirsa, M.A., Ren, M., Brantley, S.L., Sheldon, N.D., Parker, D., Schmitz, M., 2011. Neoarchean paleoweathering of tonalite and metabasalt: implications for the reconstructions of 2.69 early terrestrial ecosystems and paleoatmosphic-chemistry. Precambrian Research 189, 1–7.
Eglington, B.M., Armstrong, R.A., 2004. The KaapvaalCraton and adjacent orogens, southern Africa: a geochronological database and overview of the geological development of the craton. South African Journal of Geology 107, 13–32.
Eldridge, D.J., Greene, R.S.B., 1994. Microbiotic soil crusts: a review of their roles in soil and ecological processes in the rangelands of Australia. Australian Journal of Soils Research 32, 389–415.
Eriksson, K.A., Simpson, E.L., 1998. Controls on spatial and temporal distribution of Precambrian eolianites. Sedimentary Geology 120, 275–294.
Eriksson, P.G., Bumby, A.J., Brümmer, J.J., Van der Neut, M., 2006. Precambrian fluvial deposits: enigmatic palaeohydrological data from the c. 2–1.9 Ga Waterberg Group, South Africa. Sedimentary Geology 120, 5–53.
Eriksson, P.G., Cheney, E.S., 1992. Evidence for the transition to an Oxygen-rich atmosphere during the evolution of red beds in the Lower Proterozoic sequences of southern Africa. Precambrian Research 54, 257–269.
Eriksson, P.G., Banerjee, S., Catuneanu, O., Corcoran, P.L., Eriksson, K.A., Hiatt, E.E., Laflamme, M., Lenhardt, N., Long, D.G.F., Miall, A.D., Mints, M.V., Pufahl, P.K., Sarkar, S., Simpson, E.L., Williams, G.E., 2013. Secular changes insedimentation systems and sequence stratigraphy. Gondwana Research, http://dx.doi.org/10.1016/j.gr.2012.09.008.
Eriksson, P.G., Long, D.G.F., Bumby, A.J., Eriksson, K.A., Simpson, E.L., Catuneanu, O., Claassen, M., Mtimkulu, Mudziri, K.T., M.N., Brümer, J.J., van der Neut, M., 2008. Palaeohydrologicaldata from the 2.0–1.8 Ga Waterberg Group, South Africa: discussion of a possible unique Palaeoproterozoic fluvial style. South African Journal of Geology 111, 183–206.
Eriksson, P.G., Porada, H., Banerjee, S., Bouougri, E., Sarkar, S., Bumby, A.J., 2007. Mat-destruction features. In: Schieber, J., Bose, P.K., Eriksson, P.G., Banerjee, S., Sarkar, A., Altermann, W., Catuneanu, O. (Eds.), Atlas of Microbial Mats Features Preserved within the Siliciclastic Rock Record. Atlases in Geosciences 2. Elsevier, New York, pp. 76–105.
Eriksson, P.G., Simpson, E.L., Eriksson, K.A., Bumby, A.J., Steyn, G.L., Sarkar, S., 2000. Muddy roll-up structures in clastic playa beds of the c. 1.8 Ga Waterberg Group, South Africa. Palaios 15, 177–183.
Finkelstein, D.B., Brasseli, S.C., Pratt, L.M., 2010. Microbial biosynthesis of wax esters during desiccation: adaption of colonization of the earliest terrestrial environments. Geology 38, 247–250.
Flannery, D.T., Walter, M.R., 2012. Archean tufted microbial mats and the Great Oxidation Event: new insights into an ancient problem. Australian Journal of Earth Sciences 59, 1–11.
Fryberger, S.G., 1990. Role of water in aeolian deposition. In: Fryberger, S.G., Krystinik, L.F., Schenk, C.J. (Eds.), Modern and Ancient Aeolian Depositions: Petroleum Exploration and Production. SEPM, Denver, CO, pp. 5-1–5-11.
Fryberger, S.G., Al-Sari, A.M., Clisham, T.J., 1983. Eolian dune, interdune, and siliciclasticsabka sediments of an offshore prograding sand sea, Dhahran, Saudi Arabia. American Association of Petroleum Geologists Bulletin 67, 280–312.
Fryberger, S.G., Schenk, C.J., Krystinik, L.F., 1988. Stokes surfaces and the effects of near-surface groundwater-table on aeolian deposition. Sedimentology 35, 21–41.
Gerdes, G., Klenke, T., Noffke, N., 2000. Microbial signatures in peritidalsiliciclastic sediments a catalogue. Sedimentology 47, 279–308.
Gutzmer, J., Beukes, N.J., 1998. Earliest laterites and possible evidence for terrestrial vegetation in the Early Proterozoic. Geology 26, 263–266.
Hagadorn, J.W., Bottjer, D.J., 1997. Wrinkle structures: microbially mediated sedimentary structures common in subtidalsiliciclastic settings at the Proterozoic–Phanerozoic transition. Geology 25, 1047–1050.
Hagadorn, J.W., Bottjer, D.J., 1999. Restriction of a Late Neoproterozoic biotope: suspect-microbial structures and trace fossils at the Vendian-Cambrian transition. Palaios 14, 73–85.
Hagadorn, J.W., McDowell, C., 2012. Microbial influence on erosion, grain transport and bedform genesis in sandy substrates under unidirectional flow. Sedimentology 59, 795–808.
Hanson, R.E., Gose, W.A., Crowley, J., Ramezani, S.A., Bowring, D.S., Hall, R.P., Pancake, J.A., Mukwakwami, J., 2004. Paleoproterozoicintraplatemagmatism and basin development on the KaapvaalCraton: Age, paleomagnetism and geochemistry of ~1.93–~1.87 Ga post Waterberg dolerites. South African Journal of Geology 107, 233–254.
Heness, E.A., Simpson, E.L., Bumby, A.J., Eriksson, P.G., Eriksson, K.A., Linnevelt, S., Modungwa, T., 2012. Evidence of climatic variation within the ~2.0 Ga upper Makgabeng Formation, South Africa. Geological Society of America Abstracts with Programs 44 (7), 131.
Holland, H.D., 2002. Volcanic gases, black smokers, and the Great Oxidation Event. Geochemica et Cosmochemica Acta 66, 3811–3826.
Holland, H.D., 2006. The oxygenation of the atmosphere and oceans. Philosophical Transactions of the Royal Society B 361, 903–915.
Jansen, H., 1982. The geology of the Waterberg basin in the Transvaal, Republic of South Africa. Geological Survey of South Africa Memoir 71, 98.
Johansen, J.R., 1993. Cryptogamic crusts in semiarid and arid lands of North America. Journal of Phycology 29, 140–147.
Kenny, R., Knauth, L.P., 1992. Continental paleoclimates from δD and $\delta^{18}O$ of secondary silica in paleokarstchert lags. Geology 20, 219–222.
Kriewaldt, M., Ryan, G.R., 1967. Western Australia Geological Survey 1:250,000 Geological Series, Pyramid, Explanatory Notes: Sheet SF/50-7, pp. 1–39.
Kröner, A., Jaeckel, P., Brandl, G., Nechin, A.A., Pidgeon, R.T., 1999. Single zircon ages for granitoid gneisses in the Central Zone of the Limpopo Belt, southern Africa and geodynamic significance. Precambrian Research 93, 299–337.
Kocurek, G., Fielder, G., 1982. Adhesion structures. Journal of Sedimentary Petrology 52, 1229–1241.
Kump, L.R., Kasting, J.F., Barley, M.E., 2001. Rise of oxygen and the "upside-down" Archean mantle. Geochemistry, Geophysics, Geosystems 2, 1025–1035.
Labandeira, C.C., 2005. Invasion of the continents: cyanobacterial crusts to tree-inhabiting arthropods. Trends in Ecology and Evolution 20, 253–262.
Langford, R.P., Chan, M.A., 1989. Fluvial–aeolian interactions. Part II. Ancient systems. Sedimentology 36, 1037–1052.
Light, M.P.R., 1982. The Limpopo Belt: a result of continental collision. Tectonics 1, 325–342.
Loope, D.B., 1985. Episodic deposition and preservation of eoliansands – a Late Paleozoic example from southeastern Utah. Geology 13, 73–76.
Lowe, D.R., 1975. Water escape structures in coarse-grained sediments. Sedimentology 22, 157–204.
Malenda, H.F., Simpson, E.L., Wizevich, M.C., Tindall, S.E., 2012. Towards the recognition of biological soil crusts in the rock record: Key features from the study of modern and Cretaceous examples. In: Noffke, N., Chafetz, H. (Eds.), Microbial Mats in Sandy Deposits (Archean to Today). Society of Sedimentary Geology Special Publication 101, pp. 125–138.
Mata, S.A., Bottjer, D.J., 2009. The paleoenvironmentaldistribution of Phanerozoic wrinkle marks. Earth-Science Reviews 96, 181–195.
Meinster, B., Tickell, S.J., 1975. Precambrian aeolian deposits in the Waterberg Supergroup. Transactions of the Geological Society of South Africa 78, 191–200.
Mossman, D.J., Minter, W.E.L., Dutkiewicz, A., Hallbauer, D.K., George, S.C., Hennigh, Q., Reimer, T.O., Horscroft, F.D., 2008. The indigenous origin of Witwatersrand "carbon". Precambrian Research 164, 173–186.

Noffke, N., 2000. Extensive microbial mats and their influences on erosional and depositional dynamics of a siliciclastic cold water environment (Lower Arenigian, Montagne Noire, France). Sedimentary Geology 136, 207–215.
Noffke, N., 2009. The criteria for the biogeneicity of microbially induced sedimentary structures (MISS) in Archean and younger, sandy deposits. Earth-Science Reviews 96, 173–180.
Noffke, N., 2010. Geobiology: Microbial Mats in Sandy Deposits from the Archean Era to Today. Springer-Verlag, Berlin, pp. 194.
Noffke, N., Beukes, N., Bower, D., Hazen, R.M., Swift, D.J.P., 2008. An actualisiticpersepective into Archean worlds – (cyano-) bacterially induced sedimentary structures in the siliciclasticNhlazatse Section, 2.9 Pongola Supergroup, South Africa. Geobiology 6, 5–20.
Noffke, N., Eriksson, K.A., Hazen, R.M., Simpson, E.L., 2006. A new window into Early Archean life: Microbial mats in Earth's oldest siliciclastic tidal deposits (3.2 Ga Moodies Group, South Africa). Geology 34, 253–256.
Noffke, N., Gerdes, G., Klenke, Th., Krumbein, W.E., 1996. Microbial induced sedimentary structures–examples from modern siliciclastic tidal flat sediments. ZentralblattfürGeologie und Paleontologie 1995 (1/2), 307–316.
Noffke, N., Gerdes, G., Klenke, Th., Krumbein, W.E., 2001. Microbially induced sedimentary structures indicating climatological, hydrologically, and depositional conditions within recent and Pleistocene coastal facies zones (southern Tunisia). Facies 44, 23–30.
Noffke, N., Knoll, A.H., Grotzinger, J.P., 2002. Sedimentary controls on the formation and preservation of microbial mats in siliciclastic deposits: a case study from the Upper Neoproterozoic Nama Group, Namibia. Palaios 17, 533–544.
Ohmoto, H., 2004. The Archaean atmosphere, hydrosphere and biosphere. In: Eriksson, P.G., Altermann, W., Nelson, D.R., Mueller, W.U., Catuneanu, O. (Eds.), The Precambrian Earth: Tempos and Events. Developments in Precambrian Geology 12. Elsevier, Amsterdam, pp. 361–388.
Olsen, H., Due, P.H., Clemmensen, L.B., 1989. Morphology and genesis of asymmetric adhesion warts – a new adhesion surface structure. Sedimentary Geology 61, 277–285.
Owen, G., 1996. Experimental soft-sediment deformation: structures formed by liquefaction of unconsolidated sands and some ancient examples. Sedimentology 43, 279–293.
Owen, G., 1997. Deformation processes in unconsolidated sands. In: Jones, M.E., Preston, R.M.F. (Eds.), Deformation if Sediments and Sedimentary Rocks. Geological Society of London Special Publication 29, pp. 137–146.
Packer, B.M., 1990. Sedimentology, Paleontology, and Stable-isotope Geochemistry of Selected Formations in the 2.7-billion-year-old Fortescue Group, Western Australia. University of California, Los Angeles (Ph.D. Thesis), 187 pp.
Plüger, F., 1999. Matground structures and redox facies. Palaios 14, 25–39.
Porada, H., Bouougri, E., 2007a. Wrinkle structures – a critical review. Earth Science Reviews 81, 199–215.
Porada, H., Bouougri, E., 2007b. Wrinkle structures. In: Schieber, J., Bose, P.K., Eriksson, P.G., Banerjee, S., Sarkar, A., Altermann, W., Catuneanu, O. (Eds.), Atlas of Microbial Mats Features Preserved Within the Siliciclastic Rock Record: Atlases in Geosciences 2. Elsevier, New York, pp. 135–144.
Porada, H., Eriksson, P.G., 2009. Cyanobacterial mat features preserved in the siliciclastic sedimentary record: Paleodeserts and modern supratidal flats. In: Seckbach, J., Walsh, M. (Eds.), From Fossils to Astrobiology: Records of life on Earth and Search for Extraterrestrial Biosignatures. Cellular Origin, Life in Extreme Habitats and Astrobiology 12, pp. 181–210.
Prave, A.R., 2002. Life on land in the Proterozoic: evidence from the Torridonian rocks of northwest Scotland. Geology 30, 811–814.
Prasad, N., Roscoe, S.M., 1996. Evidence of anoxic to oxic atmospheric change during 2.45–2.22 Ga from lower and upper sub-Huronianpaleosols, Canada. Cantena 27, 105–121.
Reineck, H-.E., Gerdes, G., Claes, M., Dunajtsschik, K., Riege, H., Krumbein, W.E., 1990. Microbial modification of surface sedimentary structures. In: Heling, D. (Ed.), Sediments and Environmental Feochemistry. Springer-Verlag, New York, pp. 254–276.
Retallack, G.J., 2001. Soils of the Past: An Introduction to Paleopedology, 2nd ed. Blackwell, Oxford, pp. 600.
Retallack, G.J., 2008. Cambrian paleosols and landscapes of South Australia. Australian Journal of Earth Sciences 55, 1083–1106.
Roering, C., van Reenen, D.D., Smit, C.A., Barton Jr., J.M., De Beer, J.H., De Wit, M.J., Stettler, E.H., Van Schalkwyk, J.F., Stevens, G., Pretorius, S., 1992. Tectonic model for the evolution of the Lompopo Mobile Belt. Precambrian Research 55, 539–552.
S.A.C.S. (South African Committee for Stratigraphy), 1980. Stratigraphy of South Africa. Part 1 (Compiler L.E. Kent). Lithostratigraphy of the Republic of South Africa, South West Africa/Namibia and the Republics of Boputhatswana, Transkei and Venda. Handbook Geological Survey of South Africa 8, Pretoria, 690 p.
Schieber, J., 1998. Possible indicators of microbial mat deposits in shales and sandstones: examples from the Mid-Proterozoic Belt Supergroup, Montana, USA. Sedimentary Geology 120, 105–124.
Schieber, J., 2004. Microbial mats in siliciclastic rock record: a summary of the diagnostic features. In: Eriksson, P.G., Altermann, W., Nelson, D.R., Mueller, W.U., Catuneanu, O. (Eds.), The Precambrian Earth: Tempos and Events. Developments in Precambrian Geology 12. Elsevier, pp. 663–673.
Sheldon, N.D., 2012. Microbially induced sedimentary structures in the ca. 1100 Ma terrestrial midcontinent rift of North America. In: Noffke, N., Chafetz, H. (Eds.), Microbial Mats in Siliciclastic Depositional Systems Through Time. SEPM Special Publication 101, pp. 153–162.
Shepard, R.N., Sumner, D.Y., 2010. Unidirectional motility of filamentous cyanobacteria produces reticulate mats. Geobiology 8, 179–190.
Simpson, E.L., Eriksson, K.A., 1993. Thin eolianitesinterbedded within a fluvial and marine succession: Early Proterozoic Whitworth Formation, Mount Isa Inlier, Australia. Sedimentary Geology 87, 39–62.
Simpson, E.L., Eriksson, K.A., Kuklis, C.A., Eriksson, P.G., Bumby, A.J., Jaarsveld, C.F., 2004. Saline pan deposits, the ~1.8 Makgabeng Formation, Waterberg Group, South Africa. Sedimentary Geology 163, 279–292.
Simpson, E.L., Eriksson, K.A., Eriksson, P.G., Bumby, A.J., 2002. Eolian dune degradation and generation of massive sandstones in the PaleoproterzoicMakgabeng Formation, Waterberg Supergroup, South Africa. Journal of Sedimentary Research 72, 40–45.
Simpson, E.L., Heness, E.A., Bumby, A.J., Eriksson, P.G., Eriksson, K.A., Linnevelt, S., Modungwa, T., 2012. Implications of sandy playa deposits, ~2.0 Ga upper Makgabeng Formation, South Africa. Geological Society of America Abstracts with Programs 44 (7), 316.
Simpson, E.L., Loope, D.B., 1985. Amalgamated interdune deposits, White Sands, New Mexico. Journal of Sedimentary Petrology 55, 361–365.
Simpson, W.S., Simpson, E.L., Wizevich, M.C., Malenda, H.F., Hilbert-Wolf, H.L., Tindall, S.E., 2010. A preserved Late Cretaceous biological soil crust in the capping sandstone member, Wahweap Formation, Grand Staircase-Escalante National Monument, Utah, Palaeoclimatic implications. Sedimentary Geology 230, 139–145.
Smoot, J.P., Castens-Seidell, B., 1994. Sedimentary features produced by efflorescent salt crusts, Saline Valley and Death Valley. In: Renaut, R.W., Last, W.M. (Eds.), Sedimentology and Geochemistry of Modern and Ancient Saline Lakes. SEPM (Society for Sedimentary Geology) Special Publication 50, pp. 73–90.
Stal, L.J., 1994. Microbial mats: Ecophysiological interactions related to biogenic stabilization. In: Krumbein, W.E., Paterson, D.M., Stal, L.J. (Eds.), Biostabilization of Sediments. Biblothels- und Information-system der Carl von Ossietzky UniversitätOldenberg. (BIS)-Verlag, Oldenburg, pp. 41–53.
Tang, D.-J., Shi, X.-Y., Jiang, G., Wang, X.–Q., 2012. Morphological association of microbially induced sedimentary structures (MISS) as a paleoenvironmental indicator: An example from the Proterzoicsucession of the southern North China Platform. In: Noffke, N., Chafetz, H. (Eds.), Microbial Mats in Sandy Deposits (Archean to Today). Society of Sedimentary Geology Special Publication 101, pp. 163–175.
Thorne, A.M., Trendall, A.F., 2001. Geology of the Fortescue Group, Pilbara Craton. Geological Survey of Western Australia, Bulletin 144, Western Australia, pp. 1–249.
Sakurai, R., Ito, M., Ueno, Y., Kitajima, K., Maruyama, S., 2005. Facies architecture and sequence-stratigraphic features of the Tumbiana Formation in the Pilbara Craton, northwestern Australia: implications for depositional environments of oxygenic stromatolites during the Late Archean. Precambrian Research 138, 255–273.
Stüeken, E.F., Catling, D.C., Buick, R., 2012. Contributions to late Archeansulpher cycling by life on land. Nature Geoscience 5, 722–725.
Walraven, F., Hattingh, E., 1993. Geochronology of the Nebo granite, Bushveld Complex. South African Journal of Geology 96, 31–41.
Walter, M.R., 1984. Archeanstromatolites: Evidence of the Earth's earliest benthos. In: Schopf, J.W. (Ed.), Earth's Earliest Biosphere: It's Origin and Evolution. Princeton University Press, Princeton, pp. 187–213.
Walter, M.R., Allwood, A.C., 2005. Biosediments and biofilms. In: Selly, R.C., Cocks, L.R.M., Plimerm, I.R. (Eds.), Encyclopedia of Geology. Elsevier, Amsterdam, pp. 279–294.
Watanabe, Y., Martini, J.E., Ohmoto, H., 2000. Geochemical evidence for terrestrial ecosystems 2.6 billion years ago. Nature 408, 574–578.
West, N.E., 1990. Structure and function of soil microphytic crusts in wildland ecosystems of arid and semi-arid regions. Advances in Ecological Research 20, 179–223.
Zaady, E., Offer, Z.Y., 2010. Biogenic soil crusts and soil depth: a long-term case study from the Central Negev desert highland. Sedimentology 57, 351–358.